KÁTIA SILVA MACIEL

DESENVOLVIMENTO DE ESTRATÉGIAS DE PURIFICAÇÃO DE LACTOFERRINA E LACTOPEROXIDASE DO SORO DE LEITE

Tese apresentada à Universidade Federal de Viçosa, como parte das exigências do Programa de Pós-Graduação em Ciência e Tecnologia de Alimentos, para obtenção do título de *Doctor Scientiae.*

Orientador: Luis Antônio Minim

Coorientadores: Lizzy Ayra Alcântara Veríssimo
Valéria Paula Rodrigues Minim

VIÇOSA - MINAS GERAIS
2022

Ficha catalográfica elaborada pela Biblioteca Central da Universidade Federal de Viçosa - Campus Viçosa

T
M152d
2022

Maciel, Kátia Silva, 1990-
Desenvolvimento de estratégias de purificação de lactoferrina e lactoperoxidase do soro de leite / Kátia Silva Maciel. – Viçosa, MG, 2022.
1 tese eletrônica (46 f.): il. (algumas color.).

Orientador: Luis Antonio Minim.
Tese (doutorado) - Universidade Federal de Viçosa, Departamento de Tecnologia de Alimentos, 2022.
Inclui bibliografia.
DOI: https://doi.org/10.47328/ufvbbt.2022.176
Modo de acesso: World Wide Web.

1. Soro de leite - Processamento. 2. Separação (Tecnologia). 3. Adsorção. 4. Hidrodinâmica. 5. Leite - Proteínas. I. Minim, Luis Antonio, 1960-. II. Universidade Federal de Viçosa. Departamento de Tecnologia de Alimentos. Programa de Pós-Graduação em Ciência e Tecnologia de Alimentos. III. Título.

CDD 22. ed. 637.3

Bibliotecário(a) responsável: Alice Regina Pinto CRB6 2523

KÁTIA SILVA MACIEL

DESENVOLVIMENTO DE ESTRATÉGIAS DE PURIFICAÇÃO DE LACTOFERRINA E LACTOPEROXIDASE DO SORO DE LEITE

Tese apresentada à Universidade Federal de Viçosa, como parte das exigências do Programa de Pós-Graduação em Ciência e Tecnologia de Alimentos, para obtenção do título de *Doctor Scientiae*.

APROVADA: 03 de fevereiro de 2022.

Assentimento:

Kátia Silva Maciel
Kátia Silva Maciel
Autora

Luis Antônio Minim
Orientador

A Deus

AGRADECIMENTOS

A Deus, pela sua bondade e infinita misericórdia, pois sem ele eu não teria chegado até aqui.

Ao meu orientador Luis Antônio Minim pela orientação, apoio, pelo saber compartilhado e por todas as palavras de incentivo.

A Lizzy Ayra Alcântara Veríssimo por toda a ajuda durante o trabalho.

A todos os professores da Universidade Federal de Viçosa que contribuíram para que esse trabalho fosse realizado.

Ao Leandro Soares Santos pelos dados compartilhados.

Aos meus amigos do Laboratório de Desenvolvimento e Simulação de Processos (LADESP) e da Universidade Federal de Viçosa.

À minha família por todo o apoio.

A todos aqueles que, de alguma forma, contribuíram para que esta tese se concretizasse.

À Universidade Federal de Viçosa pela oportunidade da realização deste Doutorado.

À Coordenação de Aperfeiçoamento de Pessoal de Nível Superior – Brasil (CAPES) – pela bolsa de estudos - Código de Financiamento 001.

RESUMO

MACIEL, Kátia Silva, D.Sc., Universidade Federal de Viçosa, fevereiro de 2022. **Desenvolvimento de estratégias de purificação de Lactoferrina e Lactoperoxidase do soro de leite.** Orientador: Luis Antônio Minim. Coorientadores: Lizzy Alcântara Verissimo e Valéria Paula Rodrigues Minim.

Processos de purificação da lactoferrina e da lactoperoxidase têm sido relatados na literatura. No entanto, é apresentado um grande número de operações unitárias, alto custo dos suportes cromatográficos, baixa pureza e rendimento da molécula. Nesse sentido, a redução de etapas, a busca por novos adsorventes e, consequentemente, a redução de custos é crucial nesses processos. Além disso, a utilização de sistemas com maior porosidade oferecem alternativas por permitir a captura direta da molécula a partir de soluções particuladas e viscosas, sem a necessidade de tratamento prévio. Nesse sentido, estudar os parâmetros operacionais que afetam a porosidade do meio é determinante para otimizar as condições experimentais. A fim de melhor avaliar estes mecanismos, foram realizados estudos hidrodinâmicos e de capacidade adsortiva em colunas macroporosas de leito expandido e fixo, e posteriormente, a captura das proteínas alvo. Portanto, esse trabalho apresenta uma nova estratégia de purificação para as proteínas lactoferrina (Capítulo I) e lactoperoxidase (Capítulo II) a partir do soro de leite utilizando colunas de leito expandido e de criogel de afinidade, respectivamente. Os suportes cromatográficos analisados foram uma resina de troca catiônica Streamline SP XL e uma matriz polimérica esponjosa altamente interconectada ativada com p-aminobenzenosulfonamida para interação específica com a lactoferrina e a lactoperoxidase, respectivamente. Com o objetivo de avaliar a eficiência da separação das proteínas de cada processo, parâmetros de purificação foram investigados.

Palavras-chave: Colunas macroporosas. Propriedades hidrodinâmicas. Capacidade adsortiva. Separação. Proteínas.

ABSTRACT

MACIEL, Kátia Silva, D.Sc., Universidade Federal de Viçosa, February 2022. **Development of purification strategies for Lactoferrin and Lactoperoxidase from whey.** Advisor: Luis Antônio Minim. Co-advisors: Lizzy Alcântara Verissimo and Valéria Paula Rodrigues Minim.

Purification processes for lactoferrin and lactoperoxidase have been reported in the literature. However, a large number of unit operations, high cost of chromatographic supports, low purity and yield of the molecule are presented. In this sense, the reduction of steps, the search for new adsorbents and, consequently, the reduction of costs is crucial in these processes. In addition, the use of systems with higher porosity offer alternatives by allowing the direct capture of the molecule from particulate and viscous solutions, without the need for prior treatment. In this context, studying the operational parameters that affect the porosity of the environment is crucial to optimize the experimental conditions. In order to better evaluate these mechanisms, hydrodynamic and adsorptive capacity studies were performed in macroporous columns of expanded and fixed bed, and subsequently, the capture of the target proteins. Therefore, this work presents a new purification strategy for the proteins lactoferrin (Chapter I) and lactoperoxidase (Chapter II) from whey using expanded bed and affinity cryogel columns, respectively. The chromatographic supports analyzed were a Streamline SP XL cation exchange resin and a highly interconnected spongy polymeric matrix activated with p-aminobenzenesulfonamide for specific interaction with lactoferrin and lactoperoxidase, respectively. In order to evaluate the separation efficiency of the proteins from each process, purification parameters were investigated.

Keywords: Macroporous columns. Hydrodynamic properties. Adsorptive capacity. Separation. Proteins.

SUMÁRIO

INTRODUÇÃO

O soro de leite é o co-produto da coagulação do leite durante a produção de queijo (KHAIRE; GOGATE, 2019), representa a porção aquosa após a remoção das caseínas e gorduras do leite, e apresenta-se como um líquido opaco e de cor amarelo-esverdeado (GUIMARÃES; TEIXEIRA; DOMINGUES, 2010). O tipo e a composição química do soro variam de acordo com o queijo produzido, bem como a alimentação, criação, diferença individual de cada animal, e o clima (ALVES et al., 2014). É composto por cerca de 93% de água e 7% de lactose, proteínas, gorduras e sais minerais. Pode ser obtido em indústrias de processamento de leite ou em laboratório por três operações principais: coagulação enzimática, precipitação ácida no ponto isoelétrico das caseínas (pH = 4,6) e separação física das micelas de caseína por microfiltração (SGARBIERI, 2004).

As proteínas do soro de leite, que representam cerca de 20% das proteínas do leite, são solúveis numa vasta gama de pH, apresentam uma estrutura globular, e contêm ligações dissulfeto, que conferem um certo grau de estabilidade estrutural (AIMUTS, 2004). A qualidade nutricional das proteínas depende dos aminoácidos que as constituem, e por este critério, as proteínas do soro de leite são consideradas de elevado valor nutricional e biológico, pois são ricas em aminoácidos essenciais, sulfurados e ramificados (GALLO et al., 2022). Estas são representadas por imunoglobulinas, α-lactoglobulina, β-lactalbumina, albumina de soro bovino, lactoferrina, lactoperoxidase e glicomacropeptídeo (NATH et al., 2015).

As proteínas que estão em concentrações inferiores incluem albumina de soro bovino, lactoferrina, lisozima e lactoperoxidase (DONOVAN, 2019). Entre estas proteínas, pode-se destacar a importância da lactoferrina e da lactoperoxidase.

A lactoferrina constitui aproximadamente 1% das proteínas do soro de leite (YADAV et al., 2015), possui massa molecular de 80 kDa, apresenta alto ponto isoelétrico (8,7) e encontra-se com carga positiva no leite (POCHET et al., 2018), podendo formar complexos por meio de ligações não covalentes com outras proteínas do leite carregadas negativamente, tais como a β-lactoglobulina, albumina sérica bovina e imunoglobulina (LAMPREAVE et al., 1990), β-caseína (ANEMA; KRUIF, 2013), e com lipopolissacarídeos de membrana de glóbulo de gordura do leite (FONG; NORRIS; MACGIBBON, 2007).

Existem estudos que mostram que a lactoferrina isolada possui múltiplas propriedades funcionais e biológicas, tais como nutritivas, antimicrobianas, antivirais, anti-inflamatórias,

antioxidantes, antitumorais, e imunomoduladoras (MAYEUR et al., 2016). Quanto às suas aplicações, além de ser utilizada como ingrediente em vários alimentos, também é relatado a sua utilização em cosméticos, tais como cremes e loções de limpeza da pele e produtos de higiene bucal, como os enxaguantes bucais, géis e pastas de dente. Da mesma forma, os produtos de higiene bucal são mais frequentemente combinados com outras proteínas de defesa da mucosa, como a lactoperoxidase e a lisozima (TOMITA et al., 2002; WAKABAYASHI; YAMAUCHI; TAKASE, 2006).

A lactoperoxidase é encontrada em aproximadamente 0,5% das proteínas do soro de leite (YADAV et al., 2015), bem como nas secreções exócrinas, tais como saliva, lágrimas e vias respiratórias (MAHDI et al., 2018). Apresenta ponto isoelétrico em torno de 9,2 (ATASEVER et al., 2013) e massa molecular de 78 kDa (VAN HOOIJDONK; KUSSENDRAGER; STEIJNS, 2000). É membro das peroxidases e tem a capacidade de gerar intermediários e produtos reativos com uma ampla atividade antimicrobiana, na qual catalisa a conversão de tiocianato (SCN^-) e iodeto (I-) por peróxido de hidrogênio (H_2O_2) em hipotiocianito antimicrobiano ($OSCN^-$) e hipoiodito (IO-) (SINGH et al., 2021). Esta reação, pode provocar à ocorrência de lesões ou modificações em várias estruturas da célula (parede celular, membrana citoplasmática, sistema de transporte, enzimas glicolíticas e ácidos nucleicos) e, consequentemente, causar a morte ou inibição do crescimento ou metabolismo dos microrganismos afetados. Também é considerada um eficaz antiviral e antifúngico (URTASUN et al., 2021).

Há estudos que têm usado a lactoperoxidase para combater vários microrganismos tais como bactérias, vírus HIV-1, bolores, leveduras, protozoários, bactérias deteriorantes, bem como microrganismos patogênicos (VAN HOOIJDONK; KUSSENDRAGER; STEIJNS, 2000; SEIFU; BUYS; DONKIN, 2005; ARMENTEROS et al., 2007; PONCE, 2010). Assim, todas estas propriedades permitem que a lactoperoxidase seja utilizada em diferentes setores, tais como a indústria de leite, cosmética, farmacêutica, veterinária, agrícola, entre outras (SHARMA et al., 2013; URTASUN et al., 2017; NICOLÁS et al., 2019).

Neste contexto, devido às inúmeras propriedades que estas proteínas possuem, a obtenção de frações proteicas com um elevado grau de pureza e com uma alteração mínima da sua estrutura nativa permite que as propriedades técnico-funcionais e biológicas específicas de cada biomolécula sejam exploradas de forma mais intensiva (NICOLAI; BRITTEN; SCHMITT, 2011; NICOLAI, 2016).

Com isso, diversos suportes têm sido explorados com a finalidade de separar ambas as proteínas a partir do leite e/ou soro de leite. Para isolar a lactoferrina Urtasun et al. (2021) utilizaram quitosana com corante triazina Orange R-HE pela cromatografia em leito fixo e reportaram um rendimento de 60% com eluição em 2 etapas. Du et al. (2015) usaram a cromatografia em leito expandido com uma resina de troca catiônica Fastline SP e obtiveram uma pureza de 88,5% e recuperação de 77,1%. Ravichandran et al. (2015) utilizando dois adsorventes mercapto etil piridina (MEP HyperCel™) e fenil propil amina (PPA HyperCel™) em modo misto pela interação hidrofóbica e tiveram uma recuperação de 91% e pureza de 2.9. Teepakorn et al. (2015) usando cromatografia de troca catiônica Sartobind S75 e obtiveram uma recuperação de 80%.

Em relação a lactoperoxidase Urtasun et al. (2017) utilizando cromatografia de afnidade imobilizaram corante triazina em Sepharose 6B e verificaram seu desempenho como possível ligante em modo leito fixo. Os autores obtiveram um rendimento de 86,5% e um fator de purificação de 46,1. Pan et al. (2015) utilizaram um criogel de troca catiônica ativado com ácido 2-acrilamido-2- metil-1-propanossulfônico e reportaram uma recuperação de 92% e pureza de 98% com eluição em 3 etapas. Atasever et al. (2013) imobilizaram L-tirosina e sulfanilamida em uma matriz de Sepharose 4B ativada por brometo de cianogênio para interação específica e obtiveram um rendimento de 62,3%. Mecitoğlu et al. (2007) testaram uma resina de troca catiônica Toyopearl-SP obtendo uma pureza de 31 e recuperação de 81%.

Embora existam estudos de purificação destas proteínas, a maioria reporta um grande número de etapas, baixo rendimento e/ou pureza, alto custo do ligante e da coluna. Além disso, deve-se considerar os custos associados à natureza dos materiais que podem ser viscosos, particulados ou as proteínas estarem presentes em baixas concentrações, o que pode inviabilizar o processo, por demandarem etapas adicionais de preparo. Assim, em geral, os processos de purificação são responsáveis por cerca de 70% do custo total do processo (DYR; SUTTNAR, 1997).

Uma alternativa a esses problemas seria a utilização de técnicas cromatográficas com o desenvolvimento de novos suportes nos processos de separação, tais como leitos com maior porososidade. Tais colunas permitem a captura direta de biomoléculas, mesmo utilizando soluções particuladas e viscosas, sem que ocorra a queda de pressão (DA SILVA et al., 2022). Além disso, a existência da estrutura macroporosa proporciona baixa resistência a transferência de massa predominando o transporte convectivo e melhorando a eficiência da

separação (COIMBRA et al., 2022). Entre os materiais de baixo custo disponíveis, o leito expandido e criogel macroporoso são de grande interesse.

O leito expandido combina as propriedades hidrodinâmicas de um leito fluidizado com as propriedades cromatográficas de um leito fixo, apresentando alta porosidade depois da expansão das partículas (D'SOUZA et al., 2017), diâmetro entre 100 a 300 μm, permitindo o uso de maiores vazões. Além disso, a resina pode ser modificada em sua superfície para a sua funcionalização de acordo a adsorção da proteína alvo (ZHAO et al., 2010).

O criogel é um adsorvente polimérico, possui biocompatibilidade, acessibilidade e estabilidade mecânica (SAYLAN; DENIZLI, 2019), apresentando poros estruturais grandes interconectados da ordem de 10 a 300 μm (NEVES et al., 2020). Com a funcionalização dos mesmos, novos materiais podem ser facilmente desenvolvidos através da incorporação de ligantes específicos na matriz, permitindo a adsorção de solutos específicos (MARCUZ et al., 2021).

Portanto, o objetivo geral desse trabalho foi estudar uma nova estratégia de purificação das proteínas lactoferrina e lactoperoxidase do soro de leite a partir de colunas porosas, tais como adsorção em leito expandido e criogel de afinidade. Tais colunas foram escolhidas de acordo com as características da molécula alvo e o princípio da cromatografia a ser explorada, bem como o baixo custo destes compostos.

Além desta parte introdutória, a tese foi estruturada em 2 capítulos e as conclusões, visando o melhor detalhamento de cada um dos aspectos avaliados.

No capítulo I é apresentado o desenvolvimento de um novo processo de purificação da lactoferina, integrando dois processos: a ultrafiltração por membrana e a adsorção em leito expandido. Estudos hidrodinâmicos e de capacidade de ligação dinâmica das partículas do leito foram investigados. Afim de determinar a eficiência da separação foram avaliados os parâmetros do processo de purificação.

No capítulo II é relatado também um novo processo de purificação pelo desenvolvimento de uma nova coluna monolítica macroporosa de afinidade para captura da lactoperoxidase em uma única etapa. Estudos hidrodinâmicos e de caracterização morfológica do criogel produzido foram conduzidos. Parâmetros do processo de purificação também foram avaliados.

REFERÊNCIAS

AIMUTIS, W. R. Bioactive Properties of Milk Proteins with Particular Focus on Anticariogenesis. **The Journal of Nutrition**, v. 134, n.4, 2004.

ALVES, M. P.; MOREIRA, R. D. O.; CARLA, M.; MARTINS, D. F. Soro de Leite: Tecnologias para o Processamento de Co-produtos. **Revista Laticínio Cândido Tostes**, v. 69, n. 3, p. 212–226, 2014.

ANEMA, S. G.; KRUIF, C. G. Protein Composition of Different Sized Casein Micelles in Milk after the Binding of Lactoferrin or Lysozyme. **Journal of Agricultural and Food Chemistry**, v. 61, p. 7142−7149, 2013.

ARMENTEROS, M.; DALVIT, P.; LEYVA, V.; PONCE, P.; ALFONSO, P. Risk analysis of the exacerbation of foodborne pathogens in raw milk activated with the lactoperoxidase system. **Revista de Salud Animal**, v. 29, n. 3, p. 176–181, 2007.

ATASEVER, A.; OZDEMIR, H.; GULCIN, I.; KUFREVIOGLU, O. I. One-step purification of lactoperoxidase from bovine milk by affinity chromatography. **Food Chemistry**, v. 136, n. 2, p. 864–870, 2013.

COIMBRA, J. C.; MARTINS, M. A.; MINIM, L. A. A simplified CFD model to describe fluid dynamics, mass transport and breakthrough curves performance in cryogel supports for chromatographic separation. **Chemical Engineering Research and Design**, v. 179, p. 56-65, 2022.

DA SILVA, R. M.; GUIMARÃES, V. M.; VERÍSSIMO, L. A. A.; VIDIGAL, M. C. T. R.; MINIM, V. P. R.; MINIM, L. A. Extraction, purification by cation exchange supermacroporous cryogel and physico-chemical characterization of γ-conglutin from lupin seeds (Lupinus albus L.). **Journal of Separation Science**, v. 45, n. 2, p. 401-410, 2022.

DONOVAN, S.M. **Human Milk Proteins: Composition and Physiological Significance,** Nestle Nutrition Institute Workshop Series, 90, pp. 93-101, 2019.

D'SOUZA, R. N.; KAKARLA, P. B.; YELEMANE, V.; MEYER, R.; BOER, P. D.; FERNÁNDEZ-LAHORE, M. Controlling cell adhesion in antibody purification by expanded bed adsorption chromatography. **Separation and Purification Technology**, v. 183, p. 270–278, 2017.

DU, Q.-Y.; LIN, D.-Q.; ZHANG, Q.-L.; YAO, S.-J. An integrated expanded bed adsorption process for lactoferrin and immunoglobulin G purification from crude sweet whey. **Journal of Chromatography B**, 947-948, 201–207, 2014.

DYR, J. E.; SUTTNAR, J. Separation used for purification of recombinant proteins. **Journal**

of Chromatography B: Biomedical Applications, v. 699, n. 1–2, p. 383–401, 1997.

FONG, B. Y.; NORRIS, C. S.; MACGIBBON, A. K. H. Protein and lipid composition of bovine milk-fat-globule membrane. **International Dairy Journal**, v. 17, p. 275–288, 2007.

GALLO, V.; GIANSANTI, F.; ARIENZO, A.; ANTONINI, G. Antiviral properties of whey proteins and their activity against SARS-CoV-2 infection. **Journal of Functional Foods**, v. 89, 104932, 2022.

GUIMARÃES, P. M. R.; TEIXEIRA, J. A.; DOMINGUES, L. Fermentation of lactose to bioethanol by yeasts as part of integrated solutions for the valorisation of cheese whey. **Biotechnology Advances**, v. 28, p. 375–384, 2010.

KHAIRE, R.A.; GOGATE, P. R. Chapter 7 - whey proteins, Academic Press, pp. 193-223, C. M. B. T.-P. S. S. **Galanakis Processing and Applications**, 2019.

LAMPREAVE, F.; PIÑEIRO, A.; BROCK, J. H.; CASTILLO, H.; SÁNCHEZ, L.; CALVO, M. Interaction of bovine lactoferrin with other proteins of milk whey. **Pharmacia**, v. 12, p. 2–5, 1990.

MAHDI, L., MAHDI, N.; AL-KAKEI S.; MUSAFER, H.; AL-JOOFY, I.; ESSA, R.; ZWAIN, L.; SALMAN, I.; MATER, H.; AL-ALAK, S.; AL-OQAILI, R. Treatment strategy by lactoperoxidase and lactoferrin combination: Immunomodulatory and antibacterial activity against multidrug-resistant Acinetobacter baumannii. **Microbial Pathogenesis**, v. 114, p. 147–152, 2018.

MARCUZ, C.; ALVES MOURÃO, C.; HAUPT, K.; ALVES BUENO, S. M. Performance of phospho-L-tyrosine immobilized onto alginate/polyacrylamide-based cryogels: Effect of ligand coupling on human IgG adsorption and Fab fragments separation. **Journal of Chromatography B**, 1165, 122530, 2021.

MAYEUR, S.; SPAHIS, S.; POULIOT, Y.; LEVY, E. Lactoferrin, a Pleiotropic Protein in Health and Disease. **Antioxidants & Redox Signaling**, v. 24, n. 14, p. 813–836, 2016.

MECITOGLU, C.; YEMENICIOGLU, A. Partial purification and preparation of bovine lactoperoxidase and characterization of kinetic properties of its immobilized form incorporated into cross-linked alginate films. **Food Chemistry**, v. 104, p. 726–733, 2007.

NATH, A.; MONDAL, S.; KANJILAL, T.; CHAKRABORTY, S.; CURCIO, S.; BHATTACHARJEE, C. Synthesis and functionality of proteinacious nutraceuticals from casein whey—A clean and safe route of valorization of dairy waste. **Chemical Engineering Research and Design**, v. 97, p. 192–207, 2015.

NEVES, I. C. O.; RODRIGUES, A. A.; VALENTIM, T. T.; MEIRA, A. C. F. O.; SILVA, S. H.; VERÍSSIMO, L. A. A.; RESENDE, J. V. Amino acid-based hydrophobic affinity cryogel for protein purification from ora-pro-nobis (Pereskia aculeata Miller) leaves. **Journal of Chromatography B**, 1161, 122435, 2020.

NICOLAI, T.; BRITTEN, M.; SCHMITT, C. β-Lactoglobulin and WPI aggregates: Formation, structure and applications. **Food Hydrocolloids**, v. 25, n. 8, p. 1945–1962, 2011.

NICOLAI, T. Formation and functionality of self-assembled whey protein microgels. **Colloids and Surfaces B: Biointerfaces**, v. 137, p. 32–38, 2016.

NICOLÁS, P., FERREIRA, M. L., & LASSALLE, V. A review of magnetic separation of whey proteins and potential application to whey proteins recovery, isolation and utilization. Journal of Food Engineering, v. 246, p-7-15, 2019.

PAN, M.; SHEN, S.; CHEN, L.; DAI, B.; XU, L.; YUN, J.; YAO, K.; LIN D-Q.; YAO, S-J. Separation of lactoperoxidase from bovine whey milk by cation exchange composite cryogel embedded macroporous cellulose beads. **Separation and Purification Technology**, v. 147, p. 132–138, 2015.

POCHET, S.; ARNOULD, C.; DEBOURNOUX, P.; FLAMENT, J.; ROLET-RÉPÉCAUD, O.; BEUVIER, E. A simple micro-batch ion-exchange resin extraction method coupled with reverse-phase HPLC (MBRE-HPLC) to quantify lactoferrin in raw and heat-treated bovine milk. **Food Chemistry**, v. 259, p. 36–45, 2018.

PONCE, P. Lactoperoxidase system under tropical conditions: use, advantages and limitations in conservation of raw milk and potential applications. **Revista de Salud Animal**, v. 32, n. 3, p. 146–154, 2010.

RAVICHANDRAN, R.; PADMANABHAN, V.; VIJAYALAKHSMI, M. A.; JAYAPRAKASH, N. S. Studies on recovery of lactoferrin from bovine colostrum whey using mercapto ethyl pyridine and phenyl propyl amine HyperCel™ mixed mode sorbents. **Biotechnology and Bioprocess Engineering**, v. 20, n. 1, p. 148–156, 2015.

SAYLAN, Y.; DENIZLI, A. Supermacroporous composite cryogels in biomedical applications, **Gels**, 5, 20, 2019.

SEIFU, E.; BUYS, E. M.; DONKIN, E. F. Significance of the lactoperoxidase system in the dairy industry and its potential applications: A review. **Trends in Food Science and Technology**, v. 16, n. 4, p. 137–154, 2005.

SGARBIERI, V. C. Propriedades fisiológicas-funcionais das proteínas do soro de leite. **Revista de Nutrição**, v. 17, n. 4, p. 397–409, 2004.

SHARMA, S.; SINGH, A. K.; KAUSHIK, S.; SINHA, M.; SINGH, R. P.; SHARMA, P.; SIROHI, H.; KAUR, P.; SINGH, T. P. Lactoperoxidase: structural insights into the function, ligand binding and inhibition. **International Journal of Biochemistry and Molecular Biology**, v. 4, n. 3, p. 108–128, 2013.

SINGH, P. K.; SHARMA, P.; BHUSHAN, A.; KAUR, P.; SHARMA, S.; SINGH, T. P. Structure of a ternary complex of lactoperoxidase with iodide and hydrogen peroxide at 1.77 Å resolution. **Journal of Inorganic Biochemistry**, 220, 111461, 2021.

TEEPAKORN, C.; FIATY, K.; CHARCOSSET, C. Optimization of lactoferrin and bovine serum albumin separation using ion-exchange membrane chromatography. **Separation and Purification Technology**, v. 151, p. 292–302, 2015.

TOMITA, M.; WAKABAYASHI, H.; YAMAUCHI, K.; TERAGUCHI, S.; HAYASAWA, H. Bovine lactoferrin and lactoferricin derived from milk : production and applications. **Biochemistry and Cell Biology**, v. 112, p. 109–112, 2002.

URTASUN, N.; BAIELI, M. F.; HIRSCH, D. B.; MARTÍNEZ-CERON, M. C.; CASCONE, O.; WOLMAN, F. J. Lactoperoxidase purification from whey by using dye affinity chromatography. **Food and Bioproducts Processing**, v. 103, n. 1113, p. 58–65, 2017.

URTASUN, N.; MIGNON, A.; MARTÍNEZ-ALVAREZ, L. M.; BAIELI, M. F.; HIRSCH, D. B.; CASCONE, O.; DUBRUEL, P.; WOLMAN, F. J. Synthesis and characterization of chitosan mini-spheres with immobilized dye as affinity ligand for the purification of lactoperoxidase and lactoferrin from dairy whey. **Separation and Purification Technology**, 255, 117700, 2021.

VAN HOOIJDONK, C. M.; KUSSENDRAGER, K. D.; STEIJNS, J. M. In vivo antimicrobial and antiviral activity of components in bovine milk and colostrum involved in non-specific defence. **The British journal of nutrition**, v. 84, n. 6, p. S127–S134, 2000.

WAKABAYASHI, H.; YAMAUCHI, K.; TAKASE, M. Lactoferrin research, technology and applications. **International Dairy Journal**, v. 16, p. 1241–1251, 2006.

YADAV, J. S. S.; YAN, S.; PILLI, S.; KUMAR, L.; TYAGI, R.D.; SURAMPALLI, R. Y. Cheese whey: A potential resource to transform into bioprotein, functional/nutritional proteins and bioactive peptides, **Biotechnology Advances**, v. 33, p. 756–774, 2015.

ZHAO, J.; LIN, D.-Q.; WANG, Y.-C.; YAO, S.-J. A novel β-cyclodextrin polymer/tungsten carbide composite matrix for expanded bed adsorption: Preparation and characterization of physical properties. **Carbohydrate Polymers**, v. 80, n. 4, p. 1085–1090, 2010.

CAPÍTULO 1

Purification of lactoferrin from sweet whey using ultrafiltration followed by expanded bed chromatography

Este capítulo apresenta um novo protocolo para purificação da lactoferrina do soro de leite. Os dados experimentais deste artigo foram obtidos da Tese de Doutorado em Ciência e Tecnologia de Alimentos do Leandro Soares Santos UFV - 2013.

Artigo publicado na revista: Separation and Purification Technology
https://doi.org/10.1016/j.seppur.2020.117324.

Separation and Purification Technology 251 (2020) 117324

Contents lists available at ScienceDirect

Separation and Purification Technology

journal homepage: www.elsevier.com/locate/seppur

Purification of lactoferrin from sweet whey using ultrafiltration followed by expanded bed chromatography

Kátia Silva Maciel[a], Leandro Soares Santos[b], Renata Cristina Ferreira Bonomo[b], Lizzy Ayra Alcântara Verissimo[c], Valeria Paula Rodrigues Minim[a], Luis Antonio Minim[a,*]

[a] Federal University of Viçosa, Department of Food Technology, Viçosa, MG, Brazil
[b] State University of Southwest of Bahia, Department of Food Engineering, Itapetinga, BA, Brazil
[c] Federal University of Lavras, Department of Food Science, Lavras, MG, Brazil

ARTICLE INFO

Keywords:
Purification
Ultrafiltration
Expanded bed chromatography
Lactoferrin
Whey

ABSTRACT

Lactoferrin is an important protein found in sweet whey that has several biological activities, such as nutritional, antimicrobial, antiviral, anti-inflammatory, antioxidant, anticarcinogenic and immunomodulation. However, it is found in very low concentration in whey and its capture and purification is a challenge. This study proposes a simple strategy in which two operations for the separation and purification of lactoferrin are integrated. Sweet whey containing 0.12 mg/mL of lactoferrin was subjected to microfiltration for clarification, followed by ultrafiltration and diafiltration in order to reduce in 10 times the total volume with simultaneous concentration and pre-purification of lactoferrin to 1.1 mg/mL. In the second operation, the protein was purified by a preparative chromatography based on cationic exchange expanded bed chromatography (EBC). Adsorption isotherms were determined which allowed establishing the conditions for the chromatographic step. Hydrodynamic studies of the expanded bed and its dynamic binding capacity were also accomplished. The final concentration of the purified lactoferrin was 17.4 mg/mL, resulting in a purity of 92.7% and recovery of 87.0%.

1. Introduction

Whey is a co-product from the manufacture of cheeses and is recognized as of high nutritional and biological value, mainly attributed to proteins that are rich in sulphureted and essential branched chain amino acids [1]. Whey proteins represent approximately 20% of the total protein constituting the bovine milk. The largest fractions (70%) are β-lactoglobulin (β-lg), α-lactoalbumin (α-la) and glycomacropeptide. Albumin, immunoglobulin and subfractions such as lactoferrin, lysozyme, lactoperoxidase, among others, are present in smaller concentrations [2].

Among the aforementioned minor proteins, lactoferrin constitutes about 1% of whey proteins [3]. It's a globular glycoprotein of approximately 700 amino acid residues with a molecular weight of about 78 kDa. The protein also has a relatively high isoelectric point (pI ≈ 8.7) indicating that it is positively charged over a wide pH range, including neutral pH [4,5]. In addition to being an iron carrier, lactoferrin exerts several important biological activities, such as nutritional, antimicrobial, antiviral, anti-inflammatory, antioxidant, anticarcinogenic and immunomodulation [6,7]. All these properties outline it important to obtain lactoferrin with a high degree of purity and minimal conformational changes in its native form to allow exploring its properties for biotechnological applications.

The challenge, presented in the purification processes of lactoferrin, is the fact that high volume of whey with a very low concentration of lactoferrin (≈ 1% of the total proteins) has to be processed. Studies using one-step purification of lactoferrin are reported by [8–11]. Considering that chromatography carries the highest cost of the whole purification process, a large feed volume in that step, might meaningly increase the Unit Production Cost (UPC). Others studies reported the purification of this protein by different methods, such as affinity chromatography [12–14], cation exchance chromatography [15], filtration membrane [16,8,17] and high-gradient magnetic separation [9]. Methods that integrate unit operations using ultrafiltration and fixed bed chromatography [18] and two expanded bed chromatography [15] are also reported.

Volume reduction in the chromatographic step is crucial to reduce the UPC. Furthermore, the equipment size and process batch time are also reduced. Moreover, solution viscosity is increased, which in turn limits the use of fixed bed chromatography due to the increase in the backpressure. Also, viscosity affects mass transfer and axial dispersion that impact negatively on the dynamic capacity of the column.

* Corresponding author.
E-mail address: lminim@ufv.br (L.A. Minim).

https://doi.org/10.1016/j.seppur.2020.117324
Received 20 April 2020; Received in revised form 26 June 2020; Accepted 27 June 2020
Available online 02 July 2020

However, there is a lack of studies on how hydrodynamics and mass transfer are affected by the feed volume reduction.

The use of ultrafiltration (UF) for volume reduction and pre-purification of lactoferrin can offer an alternative. This step is important because high concentrations of other proteins can hinder the adsorption of the target protein in the chromatographic column, either by means of steric hindrance and/or competition for binding sites [19]. In the sequence of the UF, a modular process could be designed by using expanded bed chromatography (EBC). This technique is a bioseparation technology, which provides significant advantages in terms of process robustness, flexibility and economy. It can capture target proteins directly from crude raw material or viscous solutions [20–23].

Once that EBC can handle easily high liquid viscosities due to the high porosity of the bed after expansion, sample concentration by ultrafiltration that leads to an increase in the fluid viscosity is advantageous. It is known that this parameter affect porosity of the bed, as well as mass transfer and axial dispersion, hence the dynamic binding capacity (DBC) of the bed can be highly influenced by this parameter. Thus, in this study it is proposed to apply a new protocol for an effective purification of lactoferrin from bovine sweet whey. The process initially consisted in microfiltration for whey clarification, followed by ultrafiltration and diafiltration with the purpose of fluid concentration, volume reduction and pre-purification of lactoferrin, and a subsequent purification by EBC packed with cationic resin. The isotherms were determined at different pH and NaCl concentrations. Hydrodynamic studies as well as DBC of the expanded bed were investigated, considering different superficial velocities and viscosities of the fluid phase.

2. Materials and methods

2.1. Materials

Streamline SP XL cation exchanger resin was purchased from GE Healthcare (Uppsala, Sweden). Microfiltration membrane (regenerated cellulose, 0.22 um) and ultrafiltration membrane (polyethersulphone, 30 kDa) were purchased from Merck-Millipore Inc (USA). Acetonitrile (MeCN) HPLC grade and Trifluoroacetic acid (TFA) were purchased from Sigma-Aldrich (St. Louis, USA). Trifluoroacetic acid, sodium chloride, sodium phosphate (dibasic and monobasic) were purchased from Sigma-Aldrich (St. Louis, USA). Proteins standard α-la, β-lg and LF were obtained from Sigma-Aldrich. Ultrapure water was used in all experiments (Milli-Q System, Millipore Inc., USA). Fresh sweet whey was obtained from a local store.

2.2. Adsorption isotherms

The adsorption isotherms were performed in order to determine the optimal experimental conditions of pH and salt concentration for the EBC assays. The Streamline SP XL cation exchanger resin has a crystalline quartz core, spherical form, with average particle size of 200 μm and average density of 1.2 g/mL. The isotherms were investigated according to an entirely randomized factorial planning 2x5 factorial scheme, with two levels of pH (7.0 and 8.0) and five concentrations of NaCl (0, 10, 20, 40 and 80 mmol/L). The adsorption isotherms assays were carried out in batches with two repetitions.

The dried resin (25 mg) was previously conditioned for 12 h in an eppendorf tubes containing 200 μL of sodium phosphate buffer (0.05 M) with a given pH and NaCl concentration. In sequence, different volumes (0 to 1600 μL) of standard lactoferrin solution (50 mg/mL) were added in order to obtain different concentrations of protein (5 to 45 mg/mL). The tubes were shaken overnight in a rotating device at constant temperature of 25 °C. The lactoferrin concentration (before and after adsorption) in the liquid phase was determined by spectrophotometry according to the Bradford method [24]. The amount of adsorbed lactoferrin (q) was determined by mass balance (Eq. (1)).

$$q = \frac{V}{m}(C_0 - C_l) \tag{1}$$

where V is the total volume of the liquid phase (mL), m is the mass of the adsorbent (g), C_0 e C_l is the initial and final concentration of protein in the supernatant, respectively (mg/mL).

The Langmuir model was adjusted to the experimental data (Eq. (2)).

$$q = \frac{q_m C}{K_d + C} \tag{2}$$

where q (mg protein/g resin) is the lactoferrin concentration in the solid phase, k_d (mL/mg) is the dissociation constant, q_m is the apparent maximum adsorption capacity and C (mg protein/mL solution) is the concentration of lactoferrin in the liquid phase in the equilibrium condition.

2.3. Hydrodynamic properties of the expanded bed

Glycerol solutions were used for the hydrodynamic characterization of the column, and they were chosen as a viscosity modifier for the feed solution neither adsorb to the cation exchanger resin nor interfere with the light absorption of lactoferrin at a wavelength of 280 nm. Glycerol concentrations of 5, 10, 15 and 20% (v/v) in sodium phosphate buffer (0.05 M; pH 6.0) and fluid velocities of 100, 150, 200, 250 and 300 cm/h were used. The system was composed of a Streamline® 25 glass column (GE Healthcare, Uppsala, Sweden) with 25 mm of internal diameter and 100 cm height, a Masterflex® 7518–10 peristaltic pump (Cole-Parmer Instruments Co., Barrington, USA) and an UVis-920 monitor detector (GE Healthcare, USA). The column was packed with the resin to a height of 14.0 ± 0.2 cm, and the piston of the column was fixed at 5.0 cm above the height of the expanded bed. The absorbance was taken at 280 nm. The analyses were performed in triplicate.

2.3.1. Expansion degree

The Expansion degree (E_D) was determined according to Eq (3).

$$E_D = \frac{H}{H_0} \tag{3}$$

where H is the height (cm) of the bed after expansion in a given velocity and H_0 is the height (cm) of the initial bed.

2.3.2. Porosity

The porosity (Ɛ) of the bed was determined according to Eq. (4) [25].

$$\varepsilon = 1 - \frac{V_P}{V_L} = 1 - \frac{H_0}{H} \tag{4}$$

where V_P and V_L are the volumes of the packed and the expanded bed, respectively, and H_0 and H are the heights of the packed and the expanded bed, respectively.

2.3.3. Residence time distribution (RTD)

RTD was determined in order to obtain the mean residence time ($\bar{t}$) and the variance (σ^2). The RTD curves were obtained as described in the Amersham Pharmacia Biotech [26]. A mixture of glycerol and sodium phosphate buffer (0.05 M; pH 6.0) containing acetone (20% v/v) was applied to the column and the monitor response was acquired at 280 nm. The column parameters were calculated according to Eqs. (5) and (6):

$$D_{ax} = \frac{UH}{2\varepsilon\bar{t}^2}\sigma^{-2} \tag{5}$$

$$Bo = \frac{UH}{\varepsilon D_{ax}} \tag{6}$$

where $Bo(cm)$ is the Bodenstein number, $D_{ax}(cm^2/min)$ is the axial

dispersion coefficient, U is the superficial velocity (cm/h), H the height of the expanded bed and ε is the expanded bed porosity.

2.3.4. Dbc

In order to explore the effect of superficial velocity and viscosity on the DBC, experiments to obtain the breakthrough were conducted in flow rate of 100, 150, 200 and 250 cm/h and viscosities of glycerol of 1.2 and 2.0 mPa·s at temperature of 25 °C. The lactoferrin concentration (C_0= 3 mg/cm^3) was kept constant. DBC (mg/g of adsorbent) was determined at 10% of the breakthrough, according to Eq. (7):

$$DBC = QC_0 \frac{\int_0^{v_b} (1 - C)dv}{m_{ads}} \quad (7)$$

where $Q(cm^3/min)$ is the mobile phase flow rate, $v(mL)$ is the volume, $v_b(mL)$ is the break point and $m_{ads}(g)$ is the mass of the adsorbent in the column.

2.4. Capture and purification of lactoferrin by ultrafiltration followed by EBC

2.4.1. Pre-purification and concentration of lactoferrin by ultrafiltration and diafiltration

Sweet whey (20 L) was microfiltered in a Pellicon® 2 tangential filtration module (Millipore Corp., USA), using a regenerated cellulose membrane (0.22 μm), at a flow rate of 5 L/min/m^2 and a conversion rate of 30%. The pH was adjusted to 7.0 using 0.05 M sodium phosphate buffer and NaCl was added to reach the concentration of 0.4 M. In sequence, ultrafiltration was performed using the same module and a PES (polyethersulfone) membrane of 30 kDa nominal molar weight limit. The operation was adjusted for a feed flow (Q_F) and transmembrane pressure (TMP) of 5 L/min/m^2 and 140 kPa, respectively.

Whey was initially concentrated with a concentration factor (C_F) of 9. After that, the system was configured to a diafiltration mode, using the same Q_F and TMP and sodium phosphate buffer (0.05 M; pH 7.0) as a diluent. The product was diafiltered with 6 diavolumes (N). Values of C_F and N were determined in previous experiments. The diafiltered whey was stored under refrigeration for experiments of EBC. Aliquots were collected for proteins determinations and the parameters apparent sieving (S_{App}) and retention (R_{App}) were determined, according to Eqs. (8) and (9):

$$S_{App,i} = \frac{C_{P,i}}{C_{F,i}} \quad (8)$$

$$R_{App} = 1 - S_{App,i} \quad (9)$$

where $C_{P,i}$ and $C_{F,i}$ is the concentration of a given protein (α-la, β-lg or LF) in the permeate and feed, respectively.

2.4.2. Purification of lactoferrin by cationic exchange EBC

Chromatographic capture and purification of lactoferrin from the concentrated and diafiltered whey was conducted in a Streamline® 25 glass column (GE Healthcare, Uppsala, Sweden) with 25 mm internal diameter and 100 cm height, and packed with a Streamline SP XL cationic resin (14 cm bed height).

Based on the most favorable conditions obtained in previous analyses, the bed was expanded (E_D = 1.5) with the adsorption buffer (sodium phosphate 0.05 M; pH 7.0) at 100 cm/h and equilibrated with 10 column volume (CV). Then, 2 L of diafiltered whey was fed into the column and after the breakthrough formation, the column was washed with the adsorption buffer. Adsorbed protein was eluted in fixed bed mode with the elution buffer, using a stepwise gradient of NaCl (0.2 mol/L and 0.5 mol/L). Protein fractions were collected and stored for later analysis. The adsorption and elution profiles were monitored at 280 nm.

In order to evaluate the efficiency of the lactoferrin purification at each step of the process, the recovery (R_{LF}), purity (P_{LF}) and purification factor (F_{LF}) were calculated according to Eqs. (10) to (12).

$$R_{LF} = \left(\frac{m_{LF,r}}{m_{LF,f}}\right) * 100 \quad (10)$$

$$P_{LF} = \left(\frac{m_{LF,r}}{m_t}\right) * 100 \quad (11)$$

$$F_{LF} = \frac{(m_{LF,r}/m_t)_P}{(m_{LF,r}/m_t)_F} = \frac{P_{LF,P}}{P_{LF,F}} \quad (12)$$

where $m_{LF,r}$ is the mass of lactoferrin obtained after each operation, $m_{LF,f}$ is the mass of lactoferrin present in the feed solution, m_t is the total mass of protein in the solution, $P_{LF,F}$ is the purity of lactoferrin after an operation and $P_{LF,F}$ is the purity of lactoferrin in the sweet whey.

2.5. Analytical procedures

Total protein in the collected fractions was determined by the Bradford method [24] using bovine serum albumin as standard. α-la, β-lg and LF were determined by liquid chromatography (Shimadzu LC-10AD VP, Tokyo, Japan) with a diode-array detector and Shimadzu SCL-10A VP integrator-processor with two pumps and an automatic injection. A reverse phase column (C18 apHera™ Polymer; 250 mm × 4.6 mm; 5 μm particles; Supelco Analytical) was used for chromatographic separation. The separation was conducted in gradient mode (Table 1) with mobile phase A (ultrapure water with 0.1 M NaCl and 0.1% TFA; pH 2.5) and mobile phase B (acetonitrile 80% in ultrapure water), at a flow rate of 1.0 mL/min and temperature of 40 °C. A sample volume of 25 μL, previously filtered through a 0.22 μm nylon membrane (Millipore, Bedford, USA) was injected into the system and absorbance was monitored at 210 nm (modified from Zuniga et al. [27]). The proteins were quantified with a calibration curve for standard lactoferrin with concentration of 0.02 to 2.1 mg/mL.

3. Results and discussion

3.1. Adsorption isotherms

The successful use of EBC requires the correct choice of adsorbent, which depends on the interaction between the charged groups immobilized on the resin and the target biomolecule. The Streamline SP XL cationic resin was used for the assays of adsorption isotherms for lactoferrin under different pH and salt conditions, in which it is presented in Fig. 1. The Langmuir model (Eq. (2)) was adjusted to the data and the parameters of the model are shown in Table 2.

It was noted that with the increase in pH and salt concentrations, the adsorption capacity of lactoferrin decreased. As the pH rises and approaches to the isoelectric point of the lactoferrin (pH ~ 8.7) the density of positive charges of the molecule reduces. In addition, Na^+ and Cl^- ions can interact with these ionic molecules in solution and compete for the active sites of the adsorbent [28]. These factors

Table 1
Gradient of solvent B in the HPLC method used for α-la, β-lg and LF quantification.

Time (min)	Solvent B (%)
0–3	3–40
3–6	40–44
6–10	44–50
10–17	50–55
17–21	55–63
21–24	63–70
24–27	70–70
27–30	70–3

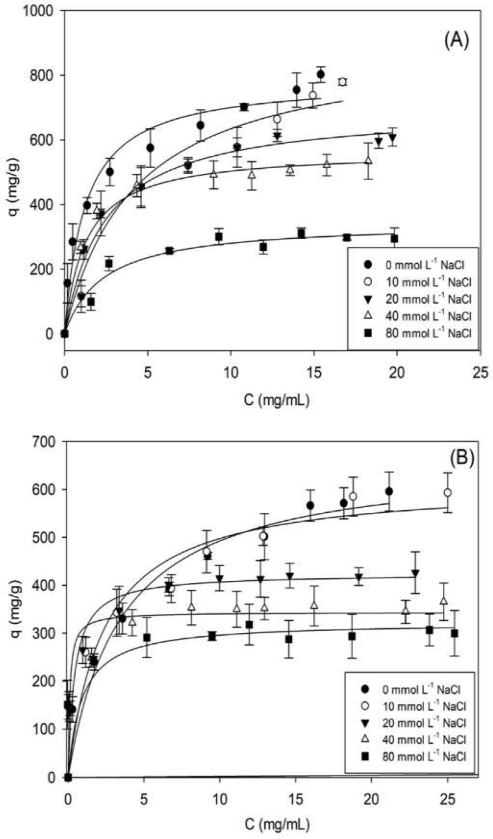

Fig. 1. Adsorption isotherms of lactoferrin on Streamline SP XL cationic resin in different concentrations of NaCl, at 25 °C (A) pH 7.0 and (B) pH 8.0.

Table 2
Adjusted parameters of the Langmuir model, at 25 °C.

pH	NaCl (mol/L)	q_m (mg/g)	K_d (mg/mL)	R^2
7.0	0.00	936.93 ± 146.36	3.10 ± 1.56	0.897
7.0	0.01	899.73 ± 75.89	4.18 ± 1.07	0.989
7.0	0.02	697.49 ± 33.85	2.41 ± 0.45	0.986
7.0	0.04	566.95 ± 47.27	1.27 ± 0.56	0.931
7.0	0.08	345.83 ± 22.24	2.34 ± 0.66	0.977
8.0	0.00	665.63 ± 43.84	3.54 ± 0.86	0.982
8.0	0.01	614.72 ± 60.75	2.35 ± 1.02	0.952
8.0	0.02	424.28 ± 9.93	0.43 ± 0.08	0.991
8.0	0.04	344.03 ± 11.00	0.11 ± 0.04	0.974
8.0	0.08	322.70 ± 35.20	0.91 ± 0.84	0.813

contribute to attenuate the electrostatic interactions between the protein and the adsorbent, whose is the driving force for adsorption. The results of maximum adsorption capacity obtained in this study (Table 2) was higher than the values obtained by Du et al. [15] when using Fastline SP cation exchanger resin for lactoferrin capture, also varying pH and ionic strength. Based on this, it is possible to assume that under the experimental conditions utilized, lactoferrin has a great adsorption capacity in Streamline SP XL cationic resin using the pH 7.0 and lower salt concentration.

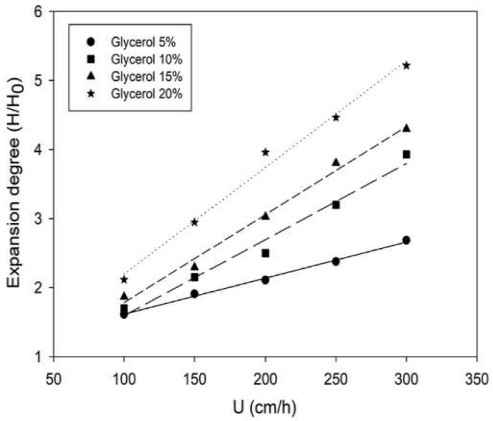

Fig. 2. Bed expansion as a function of superficial liquid velocity.

3.2. Hydrodynamic properties of the expanded bed

3.2.1. Expansion degree

Fig. 2 shows the bed expansion as a function of the superficial fluid velocity for the Streamline SP XL resin. The degree of bed expansion increased linearly with both velocity and fluid viscosity rise. The results indicate that at this range, fluidization is stable [29]. Furthermore, it was also found that the maximum operating velocity for the Streamline SP XL is 300 cm/h. It is important to know this limit because the degree of bed expansion will influence the process of protein adsorption. Above this velocity using feed solutions with 15 and 20% glycerol, an unstable interface at the top of the fluidized bed was observed, presenting large mixture with formation of preferential channels.

Bed porosity as a function of superficial velocity and glycerol concentration is shown in Table 3. The results indicate that, for most of the conditions studied, the determined porosity was within usual values (0.65 to 0.8) found in expanded bed operations. Furthermore, it also shows that flow rate and viscosity have a positive effect on the values of porosity, hence it contributes to increase mass transfer and consequently the adsorption process. It was noted that for values above 300 cm/h and 20% glycerol, there has been a great rise in porosity, in such a way that unstable interface and preferential channeling was observed.

The behavior of fluidization in the expanded bed as a function of the physical properties of particles and fluid can be analyzed by the correlation of Richardson and Zaki [30], as shown in Eq. (13). Besides, the terminal Reynolds (Re_t) and theoretical apparent terminal velocity (U_t) of the particles were determined by Eqs. (14) and (15) (Stokes Eq.), respectively.

$$u = u_t \varepsilon^n \tag{13}$$

$$U_t = \frac{d_p^2 g(\rho_p - \rho_l)}{18\mu} \tag{14}$$

Table 3
Effect of superficial velocity and glycerol concentration on expanded bed porosity.

Mobile phase (Glycerol)	ε				
	U = 100 (cm/h)	U = 150 (cm/h)	U = 200 (cm/h)	U = 250 (cm/h)	U = 300 (cm/h)
5%	0.63	0.69	0.72	0.75	0.81
10%	0.65	0.72	0.76	0.81	0.85
15%	0.68	0.74	0.80	0.84	0.88
20%	0.72	0.80	0.85	0.87	0.90

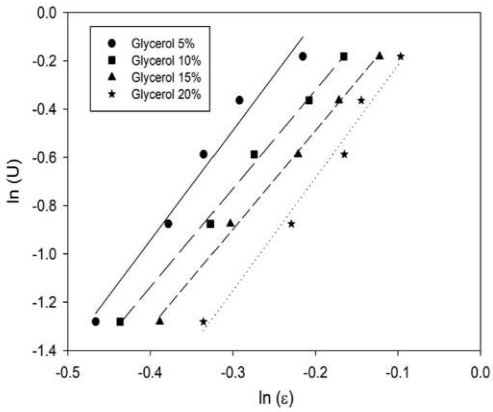

Fig. 3. Fluidization of the Streamline SP XL adsorbent in the column for different viscosities.

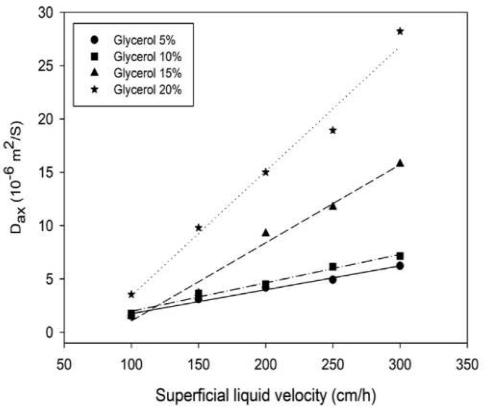

Fig. 4. Axial dispersion as a function of different velocities and viscosities at 25 °C.

$$Re_t = \frac{U_t \rho_l d_P}{\mu} \tag{15}$$

where n is the coefficient of Richardson and Zaki, u_t is the experimental apparent terminal velocity, u is the superficial velocity, ρ_p and ρ_l are the densities of the particle and the liquid, respectively, g is the acceleration of gravity, d_P is the diameter of the particle and μ is the viscosity of the liquid.

In Fig. 3 it is shown that the fluidization of the expanded bed adjusted well to Eq. (13) and its coefficients (u_t and n) were determined by linear regression. Table 4 presents the Richardson and Zaki parameters (u_t and n), as well as Re_t. It is verified that the values of u_t were in general lower than U_t indicating that stable fluidization occurs. The differences found are probably related to the particle size dispersion [31,32]. For Re in the range of $0.2 < \text{Ret} < 500$, Richardson and Zaki [30] reported that flow is laminar when values of n is in the range of 2.39 to 4.65. Thus, considering the velocities and viscosities analyzed in this study the flow is laminar, allowing stable fluidization and low backmixing.

3.2.2. Axial dispersion in the expanded bed

Fig. 4 shows the axial dispersion (D_{ax}) as a function of superficial velocity and glycerol concentration. It was observed that D_{ax} increased linearly with the increase of the fluid velocity, moreover, the growth in the glycerol concentration (or the viscosity) intensified the D_{ax} rise. As it was already shown, porosity was increased with the rise in the velocity and viscosity, which amplify both the mobility of the particles and makes axial dispersion to increase. The results observed here are in accordance to those obtained by Pålsson, Axelsson and Larsson [33] and Chen et al. [34].

Liquid mixing and bed stability can also be analyzed by means of the Bo number, which is a measure of the relationship between the convective transport and axial dispersion. It is argued elsewhere that when

Table 4
Physical properties of the fluid and Richardson-Zaki parameters as a function of glycerol concentration.

Glycerol (v/v %)	μ (mPa·s)	ρ (kg/m^3)	Apparent terminal velocity (cm/h)		n	Re_t
			U_t	u_t		
5	1.16	1007.98	3.61	2.42	4.06	0.63
10	1.40	1020.73	2.79	1.94	4.28	0.29
15	1.89	1029.75	1.96	1.39	4.39	0.21
20	2.00	1040.60	1.73	1.28	4.67	0.18

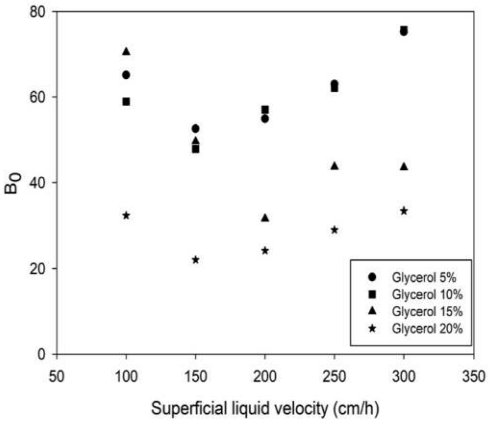

Fig. 5. Behavior of the Bo number as a function of different velocities and viscosities at 25 °C.

$B_o > 40$ the axial dispersion becomes negligible and the flow pattern is similar to plug flow [26]. In Fig. 5 the B_o number is shown for the various conditions analyzed. A decrease in its value was observed, for flow velocities up to 150 cm/h, and then it increased as velocity was raised. This occurs because the combined effect of the increase in U and H was lesser than the effect related to the growth of D_{ax}. For higher values of fluid viscosity the Bo values were lower, which means that the effect of increasing D_{ax} was more important, despite the greater expansion that occurred in the bed. According to Pålsson, Axelsson and Larsson [33] Bo increases with expansion and a possible decrease in its magnitude indicates that expansion was disturbed due to particles aggregation or even localized turbulences along the column.

3.2.3. DBC of lactoferrin in expanded bed column

DBC at C/C_0 of 10% was determined by the breakthrough curves generated through frontal analysis experiments (Table 5). The obtained values were lesser than those found in the isotherm experiments because the feed concentration to obtain the breakthrough was only 3 mg/mL and the experimental breakthroughs were not run until equilibrium. It is observed that DBC decreases from 47.44 to 24.09 mg/g as the flow rate is increased from 100 to 250 cm/h. Furthermorre, for the same flow rate (250 cm/h), DBC increased to 45.11 mg/g when viscosity was decreased from 2.0 to 1.2 mPa·s. This value is comparable when flow rate was much lower (100 cm/h). The greater is the flow

Table 5
Dynamic binding capacity at C/C_0 of 10% in different flow rate and mobile phase viscosities ($C_0 = 3mg/cm^3$).

U	μ	DBC (mg/g)
(cm/h)	(mPa·s)	
100	2.0	47.44
150	2.0	41.88
200	2.0	37.18
250	2.0	24.09
250	1.2	45.11

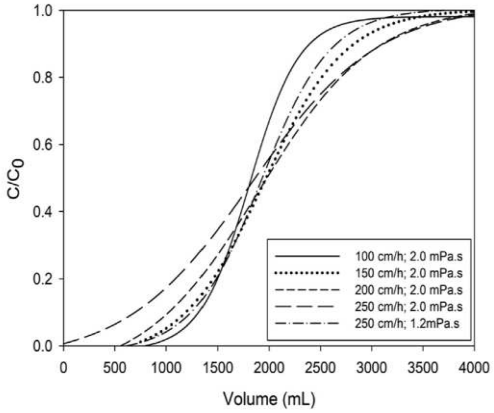

Fig. 6. Breakthrough curves of lactoferrin as a function of different flow rate and viscosities in the expanded bed column.

rate, the lesser was the residence time of solutes, which also leads to a decrease in the DBC. Nevertheless, when observing the gradient of the breakthroughs for all the conditions studied (Fig. 6), it is noticeable that the lesser the flow and viscosity, the steeper is the breakthrough and consequently, the greater is the DBC. These results can be attributed to the decrease of the axial dispersion, as it was shown before (Fig. 5).

3.3. Integration of ultrafiltration and chromatography for lactoferrin purification

3.3.1. Ultrafiltration

The protocol for lactoferrin purification proposed here involves initially the pre-purification and concentration of lactoferrin from microfiltered whey by using ultrafiltration. Concentration is important, because it will reduce the volume to be run in the subsequent chromatographic step, reducing the size of the operation. However, it is important to focus on the increase in the fluid viscosity. In fixed bed chromatography, this may cause the operation to be unfeasible. Nevertheless, EBC can work easily with viscous solution, even though axial dispersion increases (see Fig. 5) and concurrently reduces the DBC, as it was shown in Table 5. The volume of the diafiltered whey was reduced 10 times when compared to the initial sweet whey, and the viscosity of the output solution was 1.4 mPa-s, a value that could be unfeasible to process in fixed bed chromatography. This value is within the range used in the previous experiments of hydrodynamic and dynamic capacity. Thus, working with low fluid velocity will assure plug flow behavior and therefore, DBC will be higher.

The adsorption isotherms assays indicated that the most favorable experimental conditions for lactoferrin adsorption are at pH 7.0 and 0.0 mol/L of NaCl. However, to perform the ultrafiltration/diafiltration process, the ionic strength of the sweet whey was adjusted to 0.4 mol/L. According to Chaufer et al. [35], the ionic strengh in the range of 0.2 to 1 mol/L, lactoferrin is presented as tetramer, which contributes to the protein to remain in the retentate. Besides, at pH values far from the isoelectric point, β-lg preferentially presents as monomer with molar mass of 18 kDa, and may not aggregate with α-la [36]. These adjustments may contribute to a better separation of the proteins in this stage, with the proteins α-la (14 kDa) and β-lg (18 kDa) directed preferentially to the permeate, which is important because hindrance effects can be reduced in the adsorption of lactoferrin in the subsequent chromatographic step.

From the results presented in Table 6, it was possible to calculate protein retention and sieving (Eqs. (7) and (8)). The total protein retention in the ultrafiltration/diafiltration operation was 73.9%. Moreover, sieving (S_{App}) of β-lg and α-la was 36.0% and 43.5%, respectively. The values found mean that unwanted proteins exceedingly remained in the retentate with lactoferrin. These results are at the same order of the values found by Almécija et al. [36], working with a 300 kDa tubular ceramic membrane. Although about half of these proteins remained in the retentate, the use of a 30 KDa membrane prevented significative loss of lactoferrin once its retention (R_{App}) was high (90.3%). Until diafiltration step, the purification factor for the lactoferrin (F_{LF}) was 1.6, with a purity (P_{LF}) of 2.8%.

3.3.2. Cationic exchange EBC

After ultrafiltration/diafiltration, the volume to be chromatographed was reduced by 10 times, which means less time spent in the chromatographic operation and therefore, economy. Although the concentration of several proteins was reduced, the purity of lactoferrin was still low. Cationic exchange chromatography at pH 7.0 will favor, preferentially, the adsorption of lactoferrin, whose isoeletric points is around 8.7 [2]. Regarding ionic strength, the use of buffers with low molarity (0.05 mol/L in this study) is recommended to avoid competition between the buffer and the protein solution for the ion charges in the resin [37].

Fig. 7 shows the chromatographic profiles including stages of loading, washing and elution and Fig. 8 (A, B and C) presents the chromatograms of fresh whey, dialyzed whey and eluted peak. The use of stepwise gradient elution resulted in two peaks, increasing the purification factor, since the elution of contaminating proteins and the target protein occurred separately. The first peak that presented a yellow colored solution contains several proteins that were weakly adsorbed, as they were desorbed with low salt concentration (0.2 M NaCl). The second peak presented a red colored solution and it was identified as lactoferrin by the retention time on the chromatogram of Fig. 8 C. Its concentration was increased from 0.12 mg/mL in the fresh whey to 17.39 mg/mL in the eluted, which resulted in a purity of 92.7% and recovery of 87.0% (Table 6). Even using a simpler strategy of purification, these values were higher when compared to the strategy

Table 6
Parameters of the purification process. P_T: total protein.

Whey	P_T (mg/mL)	α-La (mg/mL)	β-Lg (mg/mL)	LF (mg/mL)	V (L)	R_{LF} (%)	P_{LF} (%)	F_{LF}
Fresh	6.64	1.59	2.91	0.12	20.00	100.0	1.8 ± 0.2	–
Microfiltered	5.58	1.48	2.83	0.13	18.00	97.5 ± 1.4	2.3 ± 0.1	1.3 ± 0.9
Ultrafiltered	42.54	9.06	21.91	1.13	2.00	94.2 ± 2.0	2.7 ± 0.8	1.5 ± 0.2
Diafiltered	38.57	8.17	17.33	1.07	2.00	89.2 ± 1.7	2.8 ± 0.1	1.6 ± 0.2
Eluted (Peak 2)	18.75	0.13	0.78	17.40	0.12	87.0 ± 1.5	92.7 ± 1.8	51.5 ± 0.7

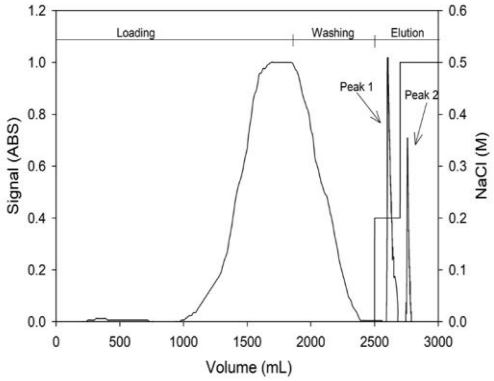

Fig. 7. Stages of the expanded bed adsorption process using the Streamline SP XL cation exchanger resin of dialyzed concentrated whey.

using two integrated fixed beds by Du et al. [15]. Also, the results were in the same order of the outcomes found by Lu et al. [18], which were obtained by using two ultrafiltration steps integrated with a fixed bed cation exchange chromatography.

4. Conclusions

In order to purify lactoferrin from whey, an integrated process based on ultrafiltration and EBC was proposed. The implementation of ultrafiltration operating in a diafiltration mode was fundamental to obtain a high degree of recovery of lactoferrin, increasing its concentration and simultaneously decreasing the total volume to be used in the chromatographic step. The isotherms followed the Langmuir behaviour and the maximum adsorption capacity was obtained at pH 7.0 and 0.0 mM NaCl. The hydrodynamic properties of the expanded bed were investigated as a function of flow rate and viscosity of the mobile phase. These variables affected negatively the DBC once the axial dispersion was increased with higher values of flow rate and viscosity. Although volume reduction during ultrafiltration is important to increase productivity of the chromatographic step, the concomitant increase of viscosity resulted in reduction of DBC. Such information is important since there is a limit to its concentration. Considering that a good recovery of 87% and a purity of 92.7% were obtained, the proposed strategy for purification of lactoferrin was successfully concluded.

CRediT authorship contribution statement

Kátia Silva Maciel: Formal analysis, Writing - original draft, Visualization. **Leandro Soares Santos:** Methodology, Investigation. **Renata Cristina Ferreira Bonomo:** Supervision, Project administration, Validation, Writing - review & editing. **Lizzy Ayra Alcântara Verissimo:** Validation, Writing - review & editing. **Valeria Paula Rodrigues Minim:** Supervision, Methodology, Writing - review & editing. **Luis Antonio Minim:** Conceptualization, Methodology, Writing - review & editing, Project administration.

Declaration of Competing Interest

The authors declare that they have no known competing financial interests or personal relationships that could have appeared to influence the work reported in this paper.

Acknowledgments

This work was supported by the Coordination of Improvement of Higher Level Personnel (CAPES). The authors would like to thank CNPq - Brasil for the financial support via grant number 304619/2017-5.

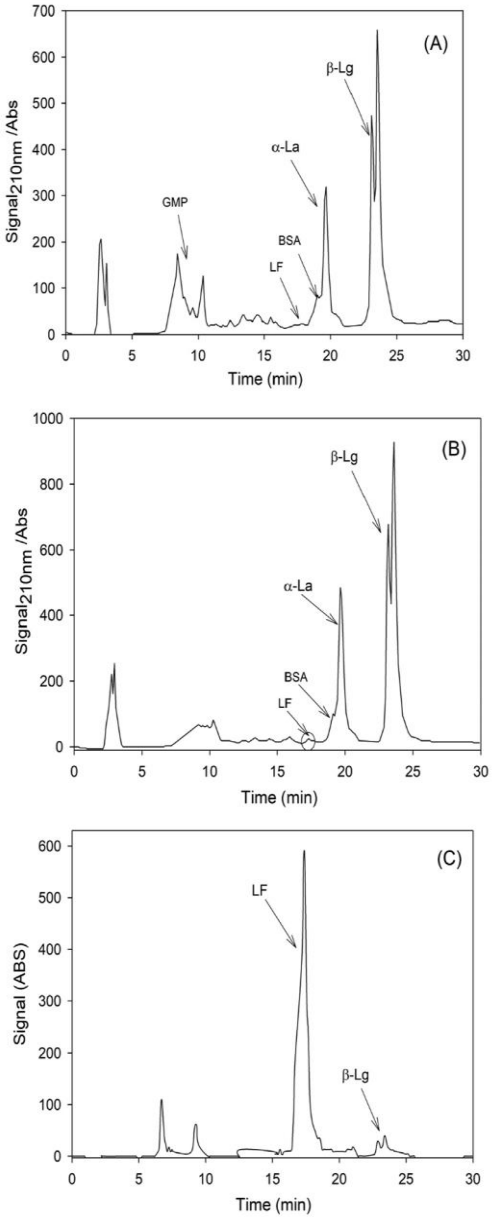

Fig. 8. Chromatographic profile (A) whey, dilution 3:10 v/v; (B) Dialyzed whey, dilution 1:20 v/v; (C) Eluted fraction at 0.5 mol/L of NaCl, 1:20 v/v.

References

[1] M.C. Devries, S.M. Phillips, Supplemental protein in support of muscle mass and health: Advantage whey, J. Food Sci. 80 (2015) A8–A15, https://doi.org/10.1111/1750-3841.12802.

[2] S. Pochet, C. Arnould, P. Debournoux, J. Flament, O. Rolet-répécaud, E. Beuvier, S. Elisa, A simple micro-batch ion-exchange resin extraction method coupled with reverse-phase HPLC (MBRE-HPLC) to quantify lactoferrin in raw and heat-treated bovine milk, Food Chem. 259 (2018) 36–45.

[3] J.S.S. Yadav, S. Yan, S. Pilli, L. Kumar, R.D. Tyagi, R.Y. Surampalli, Cheese whey: A potential resource to transform into bioprotein, functional/nutritional proteins and bioactive peptides, Biotechnol. Adv. 33 (2015) 756–774, https://doi.org/10.1016/

j.biotechadv.2015.07.002.
[4] H.Y. Li, M. Li, C.C. Luo, J.Q. Wang, N. Zheng, Lactoferrin Exerts Antitumor Effects by Inhibiting Angiogenesis in a HT29 Human Colon Tumor Model, J. Agric. Food Chem. 65 (2017) 10464–10472, https://doi.org/10.1021/acs.jafc.7b03390.
[5] W. Yang, F. Liu, C. Xu, F. Yuan, Y. Gao, Molecular interaction between (-)-epigallocatechin-3-gallate and bovine lactoferrin using multi-spectroscopic method and isothermal titration calorimetry, Food Res. Int. 64 (2014) 141–149, https://doi.org/10.1016/j.foodres.2014.06.001.
[6] M.C. Scala, M. Sala, A. Pietrantoni, A. Spensiero, S. Di Micco, M. Agamennone, A. Bertamino, E. Novellino, G. Bifulco, I.M. Gomez-Monterrey, F. Superti, P. Campiglia, Lactoferrin-derived Peptides Active towards Influenza: Identification of Three Potent Tetrapeptide Inhibitors, Sci. Rep. 7 (2017), https://doi.org/10.1038/s41598-017-10492-x.
[7] S. Mayeur, S. Spahis, Y. Pouliot, E. Levy, Lactoferrin, a Pleiotropic Protein in Health and Disease, Antioxid. Redox Signal. 24 (2016) 813–836, https://doi.org/10.1089/ars.2015.6458.
[8] C. Teepakorn, K. Fiaty, C. Charcosset, Optimization of lactoferrin and bovine serum albumin separation using ion-exchange membrane chromatography, Sep. Purif. Technol. 151 (2015) 292–302, https://doi.org/10.1016/j.seppur.2015.07.046.
[9] A. Meyer, S. Berensmeier, M. Franzreb, Direct capture of lactoferrin from whey using magnetic micro-ion exchangers in combination with high-gradient magnetic separation, React. Funct. Polym. 67 (2007) 1577–1588, https://doi.org/10.1016/J.REACTFUNCTPOLYM.2007.07.038.
[10] Q.-Y. Du, D.-Q. Lin, Z.-S. Xiong, S.-J. Yao, One-Step Purification of Lactoferrin from Crude Sweet Whey Using Cation-Exchange Expanded Bed Adsorption, Ind. Eng. Chem. Res. 52 (2013) 2693–2699, https://doi.org/10.1021/ie302606z.
[11] WO2015009400A1 - Expanded bed adsorption methods for isolation of basic milk proteins including lactoferrin - Google Patents, (n.d.). https://patents.google.com/patent/WO2015009400A1/en (accessed June 1, 2020).
[12] R. Ravichandran, V. Padmanabhan, M.A. Vijayalakhsmi, N.S. Jayaprakash, Studies on recovery of lactoferrin from bovine colostrum whey using mercapto ethyl pyridine and phenyl propyl amine HyperCel™ mixed mode sorbents, Biotechnol. Bioprocess Eng. 20 (2015) 148–156, https://doi.org/10.1007/s12257-014-0408-7.
[13] B.M.A. Carvalho, L.M. Carvalho, W.F. Silva, L.A. Minim, A.M. Soares, G.G.P. Carvalho, S.L. Da Silva, Direct capture of lactoferrin from cheese whey on supermacroporous column of polyacrylamide cryogel with copper ions, Food Chem. 154 (2014) 308–314, https://doi.org/10.1016/j.foodchem.2014.01.010.
[14] P.K. Ng, T. Yoshitake, Purification of lactoferrin using hydroxyapatite, J. Chromatogr. B. 878 (2010) 976–980, https://doi.org/10.1016/J.JCHROMB.2010.02.027.
[15] Q.-Y. Du, D.-Q. Lin, Q.-L. Zhang, S.-J. Yao, An integrated expanded bed adsorption process for lactoferrin and immunoglobulin G purification from crude sweet whey, J. Chromatogr. B. 947–948 (2014) 201–207, https://doi.org/10.1016/j.jchromb.2013.12.020.
[16] Q. Wang, G.Q. Chen, S.E. Kentish, Isolation of lactoferrin and immunoglobulins from dairy whey by an electrodialysis with filtration membrane process, Sep. Purif. Technol. 233 (2020) 115987, , https://doi.org/10.1016/j.seppur.2019.115987.
[17] S.M. Saufi, C.J. Fee, Recovery of lactoferrin from whey using cross-flow cation exchange mixed matrix membrane chromatography, Sep. Purif. Technol. 77 (2011) 68–75, https://doi.org/10.1016/j.seppur.2010.11.021.
[18] R.R. Lu, S.Y. Xu, Z. Wang, R.J. Yang, Isolation of lactoferrin from bovine colostrum by ultrafiltration coupled with strong cation exchange chromatography on a production scale, J. Memb. Sci. 297 (2007) 152–161, https://doi.org/10.1016/J.MEMSCI.2007.03.039.
[19] P.C.G. Mól, L.A.A. Veríssimo, M.R. Eller, V.P.R. Minim, L.A. Minim, Development of an affinity cryogel for one step purification of lysozyme from chicken egg white, J. Chromatogr. B Anal. Technol. Biomed, Life Sci. 1044–1045 (2017) 17–23, https://doi.org/10.1016/j.jchromb.2016.12.032.
[20] P.F. Gomes, J.M. Loureiro, A.E. Rodrigues, Expanded bed adsorption of albumin and immunoglobulin G from human serum onto a cation exchanger mixed mode adsorbent, Adsorption. 24 (2018) 293–307, https://doi.org/10.1007/s10450-018-9940-7.
[21] P. Li, P.F. Gomes, J.M. Loureiro, A.E. Rodrigues, Proteins Separation and Purification by Expanded Bed Adsorption and Simulated Moving Bed Technology, in: Contin. Process. Pharm. Manuf., Wiley-VCH Verlag GmbH & Co. KGaA, Weinheim, Germany, 2014: pp. 1–34. https://doi.org/10.1002/9783527673681.ch01.
[22] P. Li, G. Xiu, V.G. Mata, C.A. Grande, A.E. Rodrigues, Expanded bed adsorption/desorption of proteins with Streamline Direct CST I adsorbent, Biotechnol. Bioeng. 94 (2006) 1155–1163, https://doi.org/10.1002/bit.20952.
[23] P. Li, G. Xiu, A.E. Rodrigues, Experimental and modeling study of protein adsorption in expanded bed, AIChE J. 51 (2005) 2965–2977, https://doi.org/10.1002/aic.10536.
[24] M. Bradford, A Rapid and Sensitive Method for the Quantitation of Microgram Quantities of Protein Utilizing the Principle of Protein-Dye Binding, Anal. Biochem. 72 (1976) 248–254, https://doi.org/10.1006/abio.1976.9999.
[25] M.B. Dainiak, I.Y. Galaev, B. Mattiasson, Direct capture of product from fermentation broth using a cell-repelling ion exchanger, J. Chromatogr. A. 942 (2002) 123–131, https://doi.org/10.1016/s0021-9673(01)01345-0.
[26] A.P. Biotech, Ion exchange chromatography (1996), https://doi.org/10.1515/9783110862430.1187.
[27] A.D.G. Zuniga, J.S.R. Coimbra, L.A. Minim, R.C. Ferreira, Quantificação de proteínas do soro de queijo através de cromatografia líquida de fase reversa, Rev. Do Inst. Laticínios Cândido Tostes. 54 (2000) 17–21.
[28] R.A. Lira, L.A. Minim, R.C.F. Bonomo, V.P.R. Minim, L.H.M. da Silva, M.C.H. da Silva, Microcalorimetric study of adsorption of glycomacropeptide on anion-exchange chromatography adsorbent, J. Chromatogr. A. 1216 (2009) 4440–4444, https://doi.org/10.1016/j.chroma.2009.03.049.
[29] L.S. Conrado, V. Veredas, E.S. Nóbrega, C.C. Santana, Concentration of alpha-lactalbumin from cow milk whey through expanded bed adsorption using a hydrophobic resin, Brazilian J. Chem. Eng. 22 (2005) 501–509, https://doi.org/10.1590/S0104-66322005000400002.
[30] J.F. Richardson, W.N. Zaki, The sedimentation of a suspension of uniform spheres under conditions of viscous flow, Chem. Eng. Sci. 3 (1954) 65–73, https://doi.org/10.1016/0009-2509(54)85015-9.
[31] J. Thömmes, Fluidized bed adsorption as a primary recovery step in protein purification, Adv. Biochem. Eng. Biotechnol. 58 (1997) 185–230 (accessed October 12, 2019), http://www.ncbi.nlm.nih.gov/pubmed/9103914.
[32] X.-D. Tong, X.-Y. Dong, Y. Sun, Lysozyme adsorption and purification by expanded bed chromatography with a small-sized dense adsorbent, Biochem. Eng. J. 12 (2002) 117–124, https://doi.org/10.1016/S1369-703X(02)00063-3.
[33] E. Pålsson, A. Axelsson, P.O. Larsson, Theories of chromatographic efficiency applied to expanded beds, J. Chromatogr. A. 912 (2001) 235–248, https://doi.org/10.1016/S0021-9673(01)00586-6.
[34] W.-D. Chen, Y.-D. Wang, H.-H. Hu, Z.-G. Su, Hydrodynamics in an expanded bed of large size ion-exchange resin, and natural product adsorption, J. Chem. Technol. Biotechnol. 82 (2007) 135–142, https://doi.org/10.1002/jctb.1632.
[35] B. Chaufer, M. Rabiller-Baudry, D. Lucas, F. Michel, M. Timmer, Selective extraction of lysozyme from a mixture with lactoferrin by ultrafiltration, Role of the physico-chemical environment, Lait. 80 (2000) 197–203, https://doi.org/10.1051/lait:2000119.
[36] M.C. Almécija, R. Ibáñez, A. Guadix, E.M. Guadix, Influence of pH in the recovery of lactoferrin from whey with ceramic membranes, Desalination. 200 (2006) 475–476, https://doi.org/10.1016/j.desal.2006.03.401.
[37] G.V. Gautério, J. Garda-Buffon, S.J. Kalil, Single-step purification of peroxidases from rice bran: Evaluation of the main expanded-bed chromatography parameters, Ind. Crops Prod. 126 (2018) 440–448, https://doi.org/10.1016/J.INDCROP.2018.10.039.

CAPÍTULO 2

Development of an affinity cryogel for one step purification
of lactoperoxidase from whey

Este capítulo apresenta o desenvolvimento de um novo suporte cromatográfico para a purificação da lactoperoxidase do soro de leite.

Artigo a ser publicado.

Development of an affinity cryogel for one step purification of lactoperoxidase from whey

Abstract: This study proposed the development of a monolithic supermacroporous affinity column (Sulf-cryogel) for direct capture of Lactoperoxidase (LPO) from whey. Cryogel was activated using p-aminobenzenesulfonamide as ligand for specific interaction with the LPO. The activated cryogel obtained hydrodynamic and morphological properties according to the usual characteristics in the literature. The adsorptive capacity of LPO was affected by the mobile phase flow velocity, which the best condition was 0.9 cm/min. A Face Centered Design (CFD) varying pH (6, 7 and 8) and salt concentration (20, 50 and 80 mmol.L^{-1}) was used to the capture of the enzyme. Higher purification factor values were found when increasing the salt concentration and pH ($p<0.05$). There was no influence of the variables under study on the yield ($p>0.05$). These results indicate that Sulf-cryogel exhibited optimal properties as a promising chromatography support for use in high-throughput one step purification of LPO from whey.

Keywords: Enzyme, adsorption, p-aminobenzenesulfonamide, specific interaction.

1. Introduction

LPO is a glycoprotein found in milk and other exocrine secretions such as saliva, tears, and airways (MAHDI et al., 2018). It has a peptide chain of 612 amino acids, with a molecular weight of 78 KDa, a 10% carbohydrate content (VAN HOOIJDONK; KUSSENDRAGER; STEIJNS, 2000), has an isoelectric point around 9.2 and composes approximately 0.5% of whey protein (YADAV et al., 2015). It contains a heme group with one iron molecule for each protein molecule, which forms its catalytic center, and is therefore a basic protein (ATASEVER et al., 2013).

It is from the family of peroxidases (EC 1.11.1.7) (KUSSENDRAGER; VAN HOOIJDONK, 2000), which is one of the most prominent enzymes in milk and has the ability to generate reactive intermediates and products with a wide antimicrobial activity, because it catalyzes the oxidation of certain molecules, such as thiocyanate ion (SCN^-), by hydrogen peroxide (SINGH et al., 2021). It is also an effective antiviral agent and antifungal (URTASUN et al., 2021).

Due to numerous properties of this protein, obtaining its isolated form with minimal changes in its conformation and maintaining the biological activity of the molecule is essential to then be used in several applications such as food, pharmaceutical and cosmetic areas. There are studies that report the purification of this enzyme using different supports, such as chitosan with Orange R-HE triazine dye (URTASUN et al., 2021) triazine dye immobilized on Sepharose 6B (URTASUN et al., 2017), cation exchange composite cryogel embedded with cellulose beads (PAN et al., 2015), sulphanilamide and l-tyrosine to a cyanogen bromide (CNBr)-activated-Sepharose 4B matrix (ATASEVER et al., 2013) and SP-Sepharose column (MORITA et al., 2011).

Nevertheless, the enzyme purification in high level of purity and yield using minimal steps and inexpensive supports is still a chalenge. In addition, the most common difficulties result from its low concentration compared to other proteins. Moreover considering that the chromatographic techniques have high production cost, the search for the development of a new adsorbent has been oriented to the direct adsorption of the target protein, without the need for a pre-treatment of the source, such as clarification, concentration or depletion of others whey proteins prior and consequently, the operation time being reduced.

Among the materials that could be used as solid supports in these processes, macroporous cryogels for use in purification of biomolecules has considerable advantages. It consists of large pore structures, which contributes to higher mass transfer rate by convective transport, low pressure and has reduced production cost (COIMBRA et al., 2022). These properties allow direct processing of crude extracts.

Cryogels are polymeric materials synthesized by the polymerization of monomers under freezing conditions (MARCUZ et al., 2021). It presents epoxy groups on their surfaces by the addition of allyl glycidyl eter that are potential options for the immobilization of ligand groups due to theirs high reactivity and formation of covalent bonds with amine, thiol or hydroxyl groups (GONÇALVES et al., 2016). Its structure allows the immobilization of specific compounds, resulting in an affinity column. Sulphanamide compounds ($R\text{-}SO_2\text{-}NH_2$) contain an acidic nitrogen moiety, histidine and imidazole, which are heterocyclic aromatic imines (DREW, 2000). Its amino groups can react with the epoxy groups of the cryogel, becoming a ligand to LPO.

The use of these cryogels as an affinity chromatographic matrix can be powerful and generally applicable technique that is distinctly advantageous for the rapid purification of a biomolecule from a complex protein feed. Thus, for this purpose, one step purification of

LPO from whey was performed using affinity cryogel as column material in a liquid chromatography system. Initially, an affinity cryogel was prepared by adding p-aminobenzenesulfonamide as the ligand group for LPO capture. An adsorptive assay was performed in order to optimize the adsorptive capacity of LPO on the affinity cryogel, considering different flow velocities, pH and salt concentration. Studies were also conducted on the hydrodynamic and morphological characterization of the activated cryogel.

2. Materials and Methods

2.1 Materials

Acrylamide (AAm, 99%), *N,N'*-methylene-bis-acrylamide (MAAm, 99%), ammonium persulfate (APS), *N,NN',N'*-tetramethylethylene-diamine (TEMED), allyl glycidyl eter (AGE, 99%), 2,2′-azino-bis(3-ethylbenzothiazoline-6-sulfonic acid) diammonium salt (ABTS, 98%) p-aminobenzenesulfonamide (99%) were purchased from Sigma-Aldrich (St. Louis, USA). LPO and bovine serum albumin standard proteins and others chemical reagents (all of analytical grade) were also obtained from Sigma Aldrich. Ultrapure water was used in all experiments (Milli-Q System, Millipore Inc., USA).

2.2 Sulf-cryogel preparation

AAm (1.175 g), MAAm (0.325 g) and AGE (1 mL) were dissolved in deionized water to a final volume of 25 mL. The mixture was degassed for 5 min in an ultrasound bath and cooled down in ice bath. Then, 24 µl of TEMED and 100 µl of APS (27.5% m/v) were added to start polymerization. The solution was poured into plastic syringes and kept in a thermostatic bath (Model 0214M2, Quimis, Brazil) containing ethanol at −12 ºC for 24 h (Model 0214M2, Quimis, Brazil). Afterward, the column was thawed at room temperature, washed with 100 mL of deionized water and oven dried at 60 °C for 12 h (VERÍSSIMO et al., 2017).

The Sulf-cryogel was prepared by immobilizing the p-aminobenzenesulfonamide ligand on the epoxy groups of the cryogel. Initially 40 mL of 1 M HCL solution was percolated through the cryogel at a flow rate of 0.1 mL/min. After that, 1 g of p-aminobenzenesulfonamide was dissolved in 30 mL of 1 M HCL and was recirculated for 24 h utilizing the same flow rate. Subsequently, ultrapure water was pumped to remove residuals of activation agents.

2.3 Characterization of the Sulf-cryogel

2.3.1 Sweeling capacity and degree of expansion

The swelling capacity of the affinity cryogel was determined according to Savina et al. (2005). The dried cryogels of a certain weight (m_d) were immersed in 50 mL of water for 24 h. Excess water was removed from the matrices and the wet weight was measured (m_w). The swelling capacity was determined using Eq. 1.

$$S = \frac{m_w - m_d}{m_d} \tag{1}$$

The degree of expansion (mL water/g dried cryogel) was calculated according to Eq. 2. Hydrated cryogels were transferred to a graduate cylinder containing water (V_1) and the final volume (V_2) was determined (GONÇALVES et al., 2016).

$$ED = \frac{V_2 - V_1}{m_d} \tag{2}$$

2.3.2 Porosity, axial dispersion and hydraulic permeability

The analyses were performed on an Äkta Pure chromatographic system (GE Healthcare Bio-Sciences, Uppsala, Sweden) utilizing a Tricorn 10/50 glass column (GE Healthcare, Uppsala, Sweden). A UV detector monitored the corresponding peak (280 nm) at the column exit.

Residence time distribution (RTD) was measured in different flow velocities (0.3-3.8 cm/min) using acetone pulse (100 µL, 5% v/v) as a tracer and water as mobile phase. The mean residence time (t_R) and variance (σ_t^2) were obtained from the RTD curves by the momentum method using Eqs. 3 and 4, respectively. E_θ function was determined according to Eq. (5) and porosity (ε_T) was determined by linear regression of Eq. 6.

$$t_R(s) = \frac{\int_0^\infty t\, Abs\,(t)dt}{\int_0^\infty Abs\,(t)dt} \tag{3}$$

$$\sigma_t^2(s^2) = \frac{\int_0^\infty t^2 Abs\,(t)dt}{\int_0^\infty Abs\,(t)dt} - t_R^2 \tag{4}$$

$$E_\theta = t_R \frac{Abs\ (t)}{\int_0^\infty Abs\ (t)dt} \quad (5)$$

$$t_R = \varepsilon_T \frac{L}{U} \quad (6)$$

where t represent the time (min), Abs is the absorbance, L (cm) is the column length and U (cm/min) is the superficial fluid velocity.

The axial dispersion coefficients at different flow velocities were determined by non-linear regression of Eq. 7 (LEVENSPIEL, 1999) using the σ_t^2 and the ε_T of the corresponding RTD curve under closed-vessel boundary conditions.

$$\frac{\sigma_t^2}{t_R^2} = 2\left(\frac{D_{ax}}{uL}\right) - 2\left(\frac{D_{ax}}{uL}\right)^2 \left[1 - exp\left(-\frac{uL}{D_{ax}}\right)\right] \quad (7)$$

where D_{ax} is the axial dispersion coefficient and u is the interstitial fluid velocity through the column ($u = \frac{U}{\varepsilon_T}$).

Height equivalent to theoretical plate (HETP) was calculated according to Eq. 8 (GUIOCHON, 2006).

$$HETP = L\frac{\sigma_t^2}{t_R^2} \quad (8)$$

The pressure drop of the column was estimated using degassed deionized water as mobile phase at different flow velocities (0.3-3.8 cm/min). Hydraulic permeability K_w was determined by linear regression of the Darcy-Weisbach Equation in the laminar region (Eq. 9).

$$\frac{\Delta P_w}{L} = -\frac{\mu_w}{K_w} U \quad (9)$$

where ΔP_w is the pressure drop through the column (Pa), μ_w is water viscosity (Pa.s) at 25 ºC.

2.4 Fourier-transform infrared (FTIR) spectroscopy

The functional groups of the activated and pure cryogels were analyzed by Fourier transform infrared spectroscopy. Samples were read directly using the attenuated total

reflectance technique (ATR) in the infrared region of 4000 to 400 cm^{-1} with a resolution of 4 $cm \cdot min^{-1}$, using a Vertex 70 FTIR spectrophotometer (Bruker, USA).

2.5 Scanning electron microscopy

Macroporous structure and pore sizes of the Sulf-cryogel were evaluated using an scanning electron microscope (LEO 1430 VP, Zeiss, Jena, Germany) operated at 15 kV. A small sample cut from the center of the dried cryogel was coated with a layer and the gel structure was examined (LAEMMLI, 1970).

2.6 Chromatography capture

2.6.1 Effect of flow velocity on LPO adsorption from aqueous solution

Adsorption assays were performed in order to determine the optimal experimental condition of the flow velocity, for which values of (0.3-1.3) cm/min were tested.

Chromatographic capture was conducted in a Tricorn 10/50 glass column (GE Healthcare, Chicago, USA) containing the activated cryogel. Initially, the Sulf-cryogel was equilibrated with 4 column volume (CV) of phosphate buffer solution (25 mM, pH 6.8) and 100 µL of standard LPO solution (1 mg/mL) was injected through the column. After adsorption, LPO enzyme was eluted with 4 CV of equilibrium buffer added of 1 M NaCl. The Sulf-cryogel was regenerated by applying 4 CV of the equilibrium buffer for complete removal of salt.

The experiment was performed in 3 repetitions using an Äkta Pure chromatographic system (GE Healthcare Bio-Sciences, Uppsala, Sweden) at room temperature. The adsorption and elution profiles were monitored at 210 nm.

2.6.2 One step purification of LPO from whey

Whey was produced in the laboratory according to the manufacturer's conditions. Chymosin was added to skim milk for coagulum formation during 30 min at 45°C. Afterwards, whey was filtered using a cellulose acetate membrane (0.22 µm) and prepared according to the CFD shown in Table 1, which varied pH (6, 7 and 8) and salt concentration (20, 50 and 80 $mmol.L^{-1}$). The assays were conducted at flow velocity of 0.9 cm/min, based on the most favorable condition obtained in the previous analysis.

Sulf-cryogel was equilibrated with 4 CV of sodium phosphate buffer solution, varying pH and salt concentration. Then, 15 mL of whey was fed into the column and after it was

washed with 4 CV of equilibrated buffer. Elution was performed with 4 CV of equilibrated buffer added of 1 M NaCl. The collected fractions were stored for later analysis.

2.7 LPO activity

This method is based on the oxidation of ABTS as a chromogenic substrate by H_2O_2. One unit of enzyme (U) is defined as the amount of enzyme catalyzing the oxidation of 1 µmol of ABTS min^{-1} at 298 K. Briefly, 100 µL of ABTS (1 mM) in citrate-phosphate buffer (0.05 M, pH 5.0) was mixed with 10 µL of sample and 10 µL of H_2O_2 solution (30%). A calibration curve was used to quantify the samples, using LPO standard. The absorbance was measured at 405 nm at 25 ºC after 5 min of reaction (Modified from Jacob et al., 1998).

Total protein (P_T) was determined according to Bradford method (1976) using bovine serum albumin as standard.

The adsorption yield (Y%) and purification factor (P_F) were calculated by Eqs. 10 and 11:

$$Y = \frac{A_{T_e}}{A_{T_i}} \tag{10}$$

where A_{T_e} is the total activity recovered in the eluted (U) and A_{T_i} is the total activity of the whey injected (U).

$$P_F = \frac{A_{S_e}}{A_{S_i}} \tag{11}$$

where A_{S_e} is the specific activity of the eluted (U/mg) and $A_{S_i}$is the specific activity of the whey injected (U/mg).

2.8 SDS-PAGE

Sodium dodecyl sulphate polyacrylamide gel electrophoresis (SDS–PAGE) was utilized to evaluate the purity of the eluates. Electrophoresis was performed for 6 h at 100 V using a vertical gel electrophoresis system (BioRad, CA, USA) and with a 30% polyacrylamide gel. Coomassie brilliant blue R250 (0.27% (w/v) in acetic acid:water:methanol (1:2.4:4, v/v/v) was used as the staining solution and the gel was destained using acetic acid:methanol:water (1:4.3:9, v/v/v) solution (LAEMMLI, 1970).

2.9 Experimental Design and Statistical Analysis

The parameters were evaluated using analysis of variance (ANOVA) at a 5% level of significance. The results were subjected to regression analysis, and a quadratic polynomial model was fitted. The adequacy of the model was determined by evaluating the lack of fit, coefficient of determination (R_2), and Fisher's test (F-value) obtained from the analysis of variance. The Student's t-test was performed for each estimated parameter.

3. Results and Discussion

3.1 Characterization of the affinity cryogel

The morphological and hydrodynamic properties of the cryogel determine the efficiency of the interaction between the immobilized ligand and the target biomolecule. Cryogel was synthesized by cryopolymerization of AAm as a functional monomer with MAAm in the presence of AGE. p-aminobenzenesulfonamide was attached to the epoxy groups on the cryogel in order to obtain the Sulf-cryogel.

Fig. 1 shows the infrared absorption spectra of the pure and activated cryogels. It was verified that the activated cryogel presented a wider and higher band than pure cryogel at 3100-3600 cm^{-1}, which indicates the presence of water (O-H) and stretching vibrations of –N-H (MÓL et al., 2019; TAO, SUN et al., 2014). This evidences the immobilization of the p-aminobenzenesulfonamide ligand on the cryogel, since the epoxy groups of the cryogel react with the amino group of the ligand.

A longer infrared absorption band is also observed at 1600-1680 cm^{-1}, which are characteristic of C=C (JING et al., 2019, VAN NIEKERK et al., 2008) and the peak observed at 1440 cm^{-1} is associated to bending vibration of C–H, both from the aromatic ring of the ligand (JAIN; BAJPAI; BAJPAI, 2017; BARBOSA, 2007). The absorption bands at 1315-1350 cm^{-1} are attributed to S=O stretching vibration from the sulfonamides (BARBOSA, 2007).

The swelling capacity was characterized as the amount of water absorbed by dry cryogel and the degree of expansion by the difference between the mass of the dehydrated and hydrated cryogel, presenting the values of 11.43 ± 0.5 g/g and 16.26 ± 0.3 mL/g, respectively. These analyses show that the cryogel mass occupies a large volume when hydrated, reinforcing the nature of the pores of its structure, as well as a sponge and elastic characteristic and consistent, confirming what several authors have reported for other types of

activated cryogels (NEVES et al., 2020; DE OLIVEIRA et al., 2019; MÓL et al., 2019; YAO et al., 2006).

The existence of the pores was also observed by scanning electron microscopy (Fig. 2). It is noted that the matrices are formed by a uniform structure with interconnected pores and diameters ranging from 20 to 100 μm.

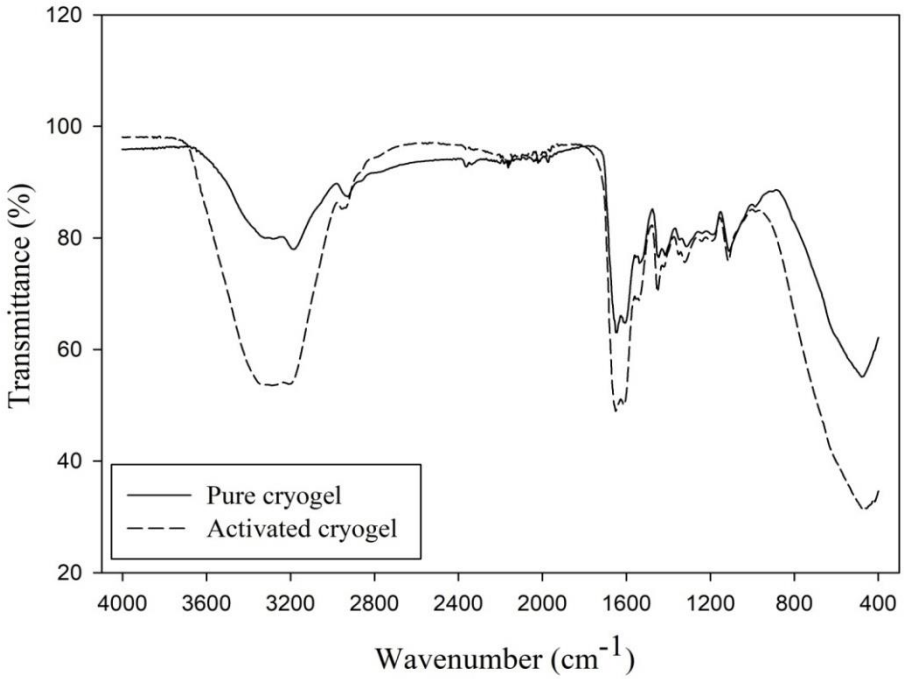

Fig. 1. Infrared absorption spectra of the pure and activated cryogels.

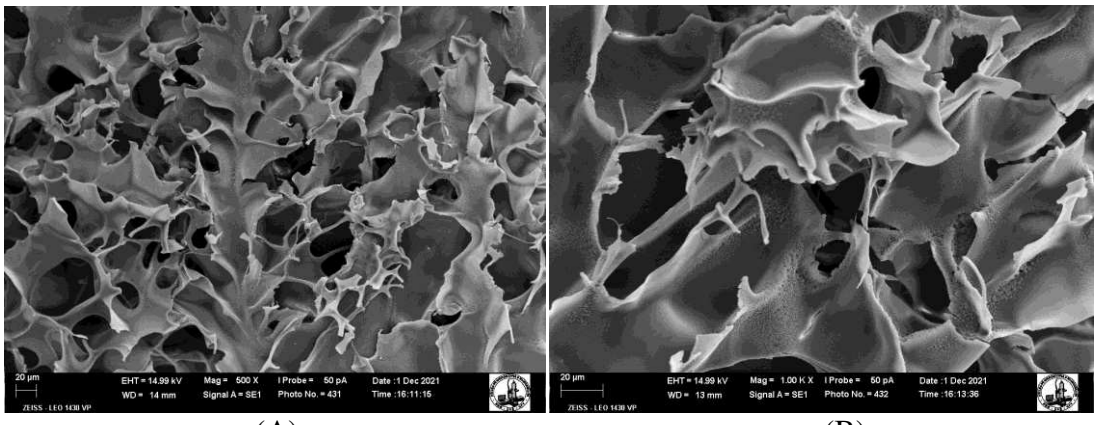

(A) (B)

Fig. 2. SEM micrograph of Sulf-cryogel. (A) 500x (B) 1000x.

Fig. 3 presents the distribution of a tracer for the different conditions evaluated. It was verified that RTD did not vary at the different flow velocities (Fig. 3). The results showed symmetrical peaks, indicating low dispersion, representing a piston-like flow profile.

From the RTD curves, the mean residence time and variance were calculated using the momentum method, which the D_{ax} and HEPT were determined. D_{ax} increased with increasing mobile phase flow velocity (Fig. 4) and the porosity (ε_t =0.96) was determined by linear regression (Eq. 3). These values are within the range obtained in experiments with macroporous cryogels (PAN et al., 2015; YE et al., 2013).

As well as D_{ax}, HETP is also determined in order to verify the performance of the column. It can be verified that there was no variation of HETP as a function of flow velocity (Fig. 5), which indicates that the mass transfer to occur predominantly by convection. This behavior is similar to the studies reported by the authors Mol et al. (2019) and Neves et al. (2020).

The experimental data pressure drop as a function at different flow velocities are shown in Fig. 6. The hydraulic permeability was calculated by Darcy-Weisbach Eq. (6) (K_w = 2.51x10^{-13} m^2), which is a result close to other polyacrylamide cryogels reported by Mól et al. (2019), Fontan et al. (2018), Mól et al. (2017) and Carvalho et al. (2014). This value is related to the resistance to flow through the activated cryogel and it is considered low, compared to fixed bed columns. The pressure drop, as well as pore structure contributes to increase mass transfer and, consequently, the adsorption process, thus enhance the separation efficiency (MACIEL et al., 2020). With this, it can be inferred that the presence of large pores and its highly porous structure, as shown in Fig. 2, allow the unobstructed passage of viscous or particulate solutions, as mentioned before.

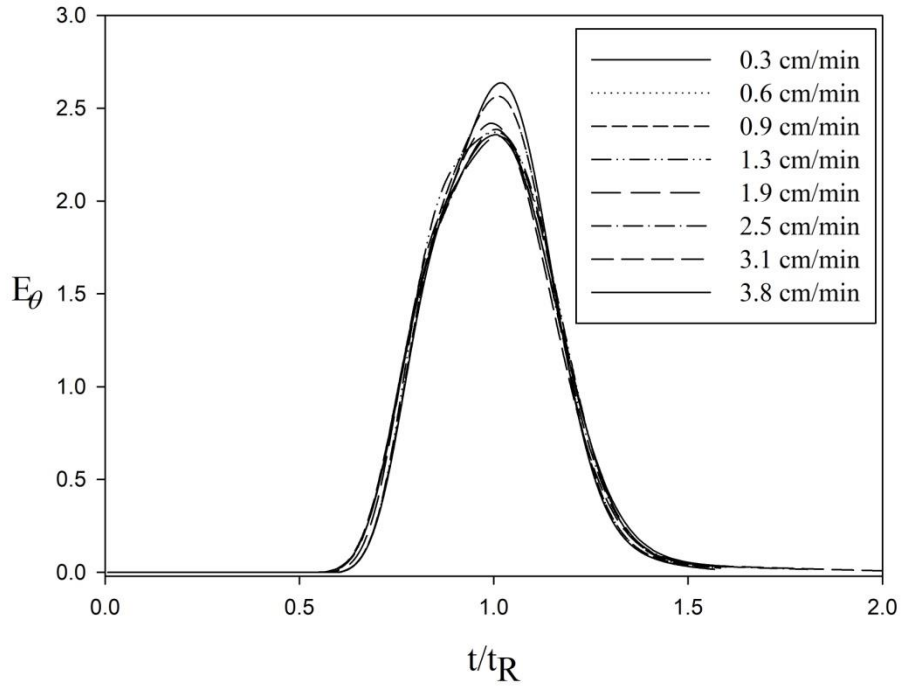

Fig. 3. RTD curves at different mobile phase surface velocities through the affinity cryogel column.

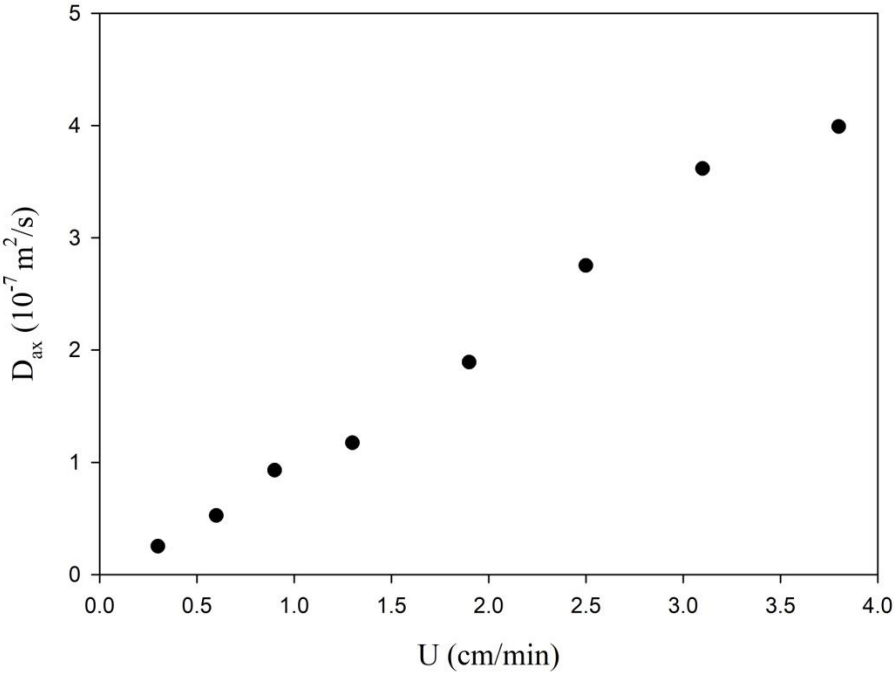

Fig. 4. Axial dispersion coefficients (D_{ax}) at different mobile phase surface velocities through the affinity cryogel column.

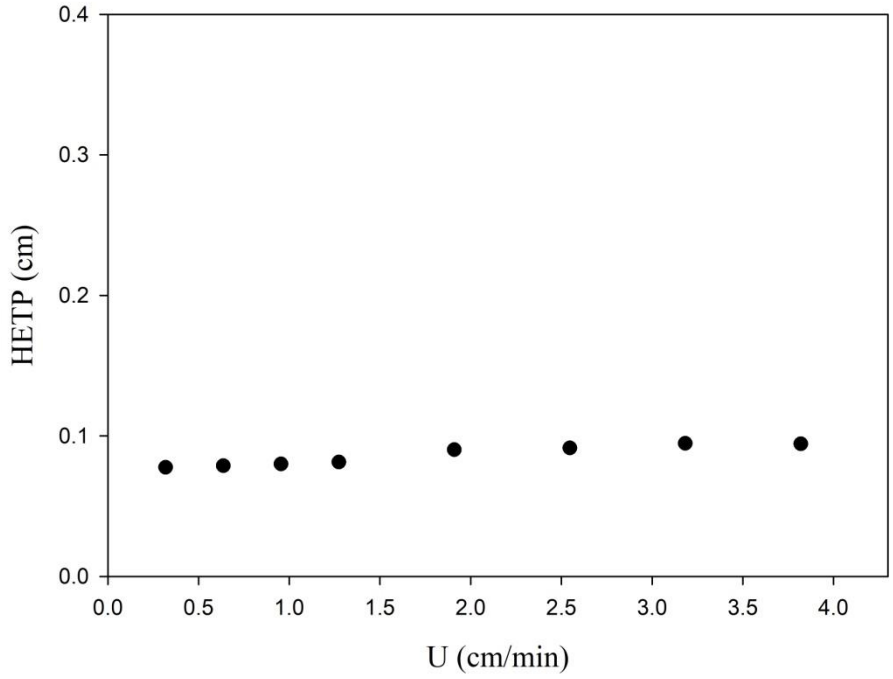

Fig. 5. HETP as a function of mobile phase at different flow velocities.

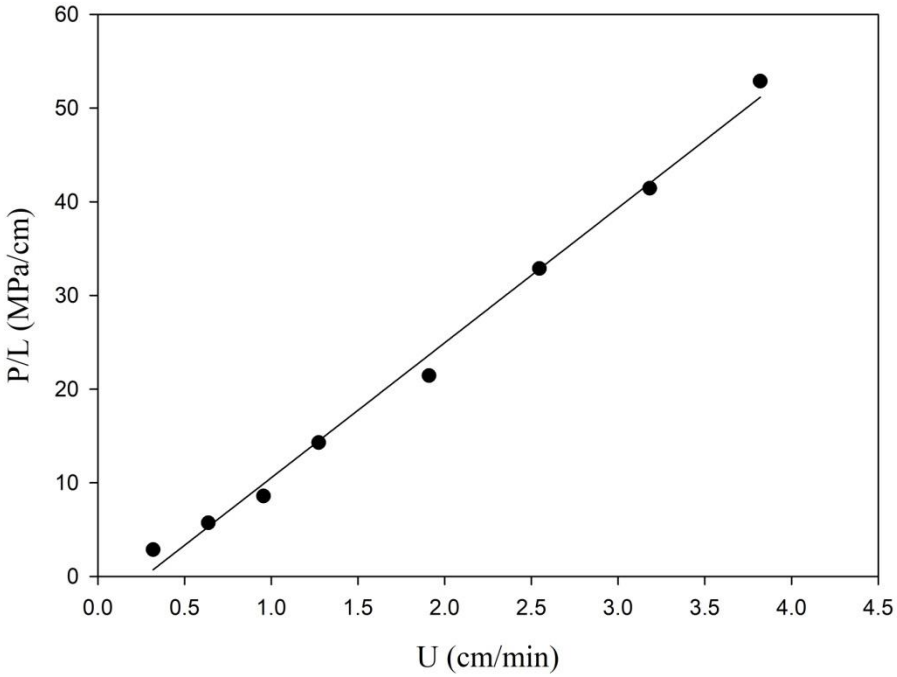

Fig. 6. Experimental data of pressure drop at different mobile at different flow velocities and adjusted equation to determine permeability (−).

3.2 Chromatography capture

3.2.1 Effect of flow velocity on the adsorbed LPO in affinity cryogel

Several analogs of sulfonamide have been demonstrated to possess good binding affinities for LPO (ATASEVER et al., 2013). According to this, in the present study the affinity cryogel was synthesized through the coupling of the p-aminobenzenesulfonamide ligand.

Adsorption of the LPO standard was tested using a Sulf-cryogel as column material in a liquid chromatography system. Fig. 7 shows the experimental results of adsorbed LPO concentration as a function of different flow velocities. It was verified that there was a tendency to increase the adsorbed LPO concentration up to 0.9 cm/min, but thereafter it decreased. This behavior can be explained by the higher mass transfer of the solute through the column pores when higher velocities are used. However, the concomitant increase is undesirable, as observed in the flow velocity at 1.3 cm/min, since the residence time becomes low, decreasing the interaction of the LPO and bind to the ligand groups, in addition, an increase in axial dispersion occurs, decreasing the efficiency of the column, as mentioned before (Fig. 4).

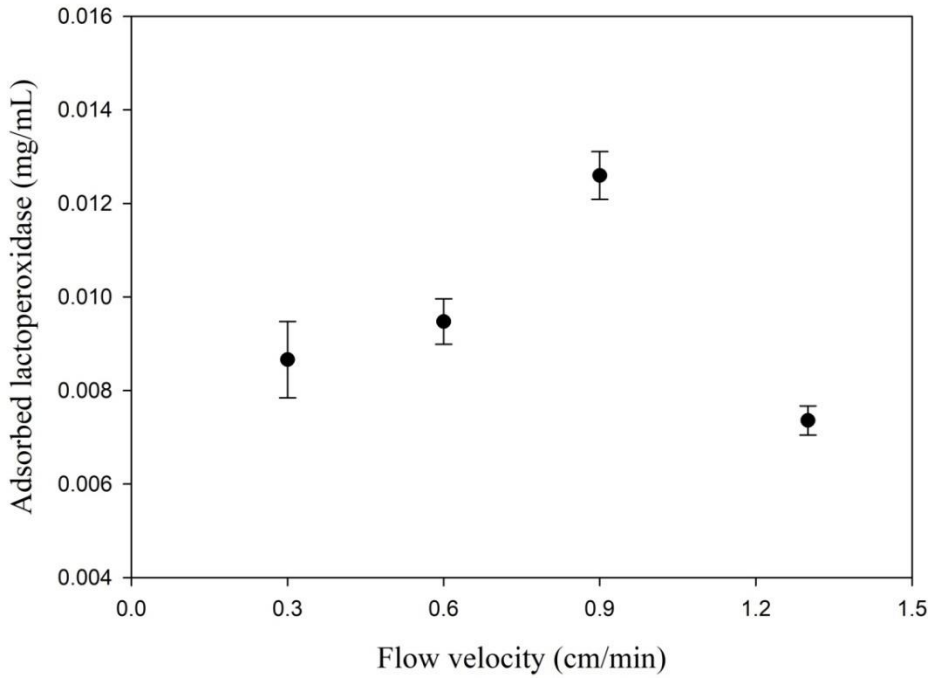

Fig. 7. Effect of flow velocity on LPO adsorption in affinity cryogel.

3.2.2 One step purification of LPO from whey

A CFD was then conducted to determine P_F and Y as a function of the variables salt concentration and pH (Table 1). The solutions were pumped through the column at 0.9 cm/min, since it was the best flow velocity, as mentioned before (Fig. 7). According to the ANOVA, it was verified that the variables under study exercised significant influence ($p<0.05$) for P_F, presenting significant model ($p<0.05$) and no significant lack of fit ($p>0.05$) and a coefficient of determination of 92.94% (Eq. 12). However, the effect of the variables was not significant ($p>0.05$) for Y.

$$P_F = 1299 + 0.506\, x_1 + 362\, x_2 - 22.91\, x_2^2 \quad (12)$$

Fig. 8 shows the chromatographic profile obtained after whey loading, washing and elution. Note that eluted fraction showed a single peak corresponding to LPO which was confirmed by the enzymatic activity analysis (Table 1) and SDS-PAGE (Fig. 10). This demonstrated the specificity of the produced ligand with the p-aminobenzenesulfonamide to the enzyme. The LPO protein has a molecular weight of 80 kDa. The standard (Lane 3) migrated at a similar distance to the LPO purified from whey (Lane 4) and localized close to 75 KDa of the molecular marker (Lane 2).

From the results presented in Table 1, whey feeding solution presented P_T of 3.25 mg/mL and LPO A_S of 2.44 U/mg. After purification, the highest values of P_F were obtained with increasing pH and salt concentration (Fig. 9), possibly due to a greater shielding of the charges of the protein by the salt, decreasing the electrostatic interaction. Thus, within the range studied, the best condition for adsorption of LPO was using the salt concentration of 80 $mmol.L^{-1}$ and pH 8 (Table 1). In addition, although the Y was non-significant, it was 100%, presenting a higher activity.

Even using a simple strategy of purification, these values were higher when compared with other authors. Urtasun et al. (2021) and Urtasun et al. (2017) report in two studies using Reactive Red 4-Sepharose matrix in batch mode for LPO purification showed Y (%) of 86.5 and P_F of 46.1. Atasever et al. (2013) utilized a Sepharose 4B-L-tyrosine-sulfanilamide affinity matrix for the purification of LPO from whey, in a single step elution, but 62.3% of LP was recovered. Pan et al. (2015) report high purity and recovery over 90% using a cation exchange composite cryogel embedded with cellulose beads in 3 elutions. Chiu and Etzel

(1997) utilized cation exchange membrane for LPO isolation from whey. The authors showed that high purity LP can be obtained by gradient elution, but the recovery was 73%.

However, the low concentration of LPO in whey makes affinity chromatography using cryogel an interesting one-step purification option, since the results of this study demonstrate the specificity of the affinity cryogel with highly specific interactions between the enzyme and the ligand, which the purity degree proves.

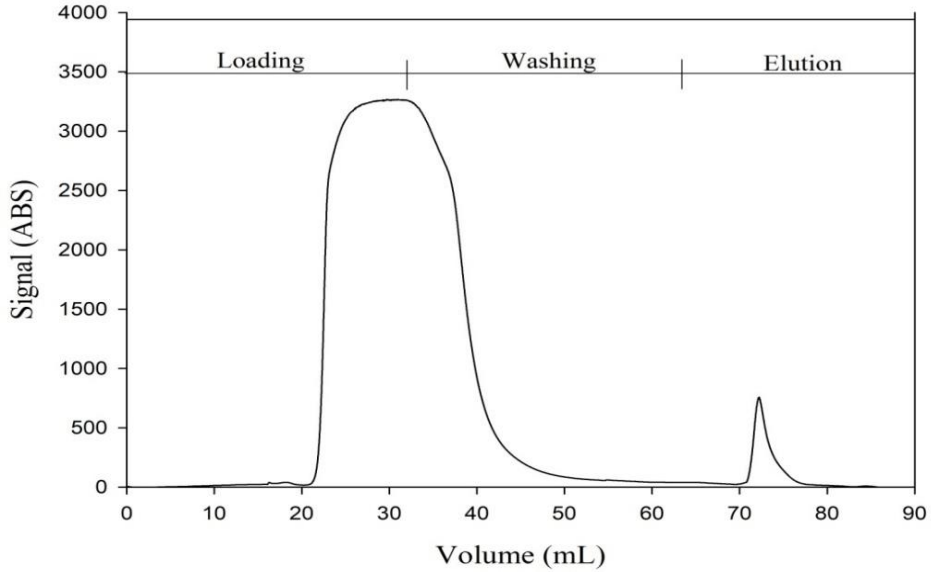

Fig. 8. Adsorption profile of LPO purification from Whey.

Table 1. Experimental conditions of the design CFD and obtained results of total protein content (P_T), total activity (A_T), specific activity (A_S), purification factor (P_F) and yield (Y) of LPO in the whey and eluted sample.

Assay	P_T (mg/mL)	A_T (U)	A_S (U/mg)	P_F	Y (%)
Feed	3.2512	7.9571	2.4483	1	100
Eluted	0.0065	8.9010	430.6252	175.8849	111.8620

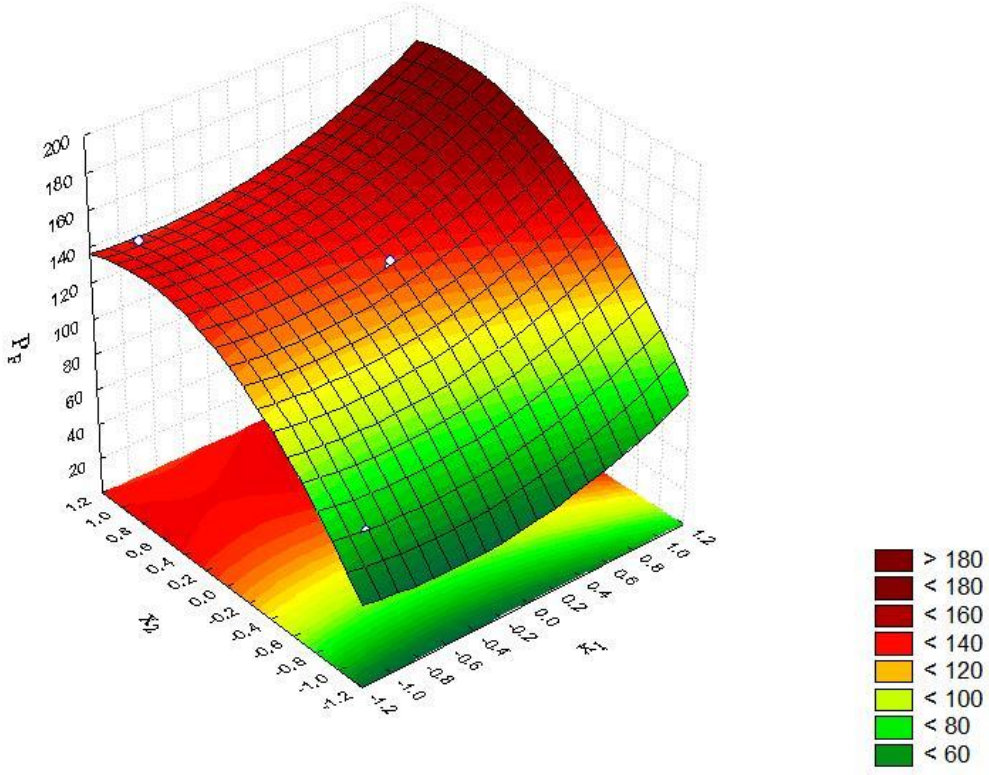

Fig. 9. Surface response graph of the P_F as a function of the salt concentration (x_1) and pH (x_2).

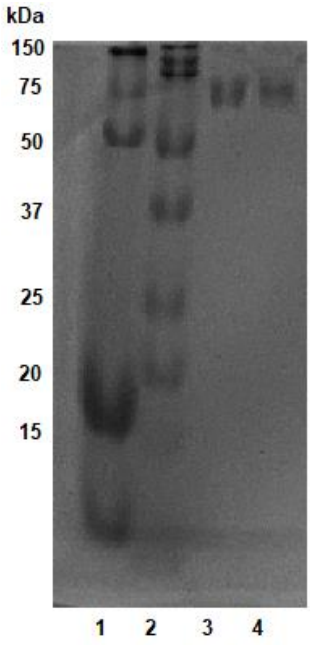

Fig. 10. SDS-PAGE analysis of chromatographic purification process of LPO from whey by affinity cryogel in one step. Lane 1: Feed solution of whey; Lane 2: Molecular marker; Lane 3: Standard LPO (1 mg/mL); and Lane 4: peak fraction from elution of feed solution of whey (CFD).

4. Conclusions

This study demonstrated a successful purification method for LPO, using an affinity cryogel in a single step. The development of a new support with immobilized p-aminobenzenesulfonamide aimed at the direct adsorption of the enzyme even at low concentration and without the need for a pre-treatment of the source. The successful functionalization of the cryogel with the ligand can be confirmed by FTIR.

The Sulf-cryogel showed desirable properties such as high porosity, low dispersion and low flow resistance. HETP also was low and not dependent of flow velocity.

The best condition of the standard LPO adsorption was defined as 0.9 cm/min. The results presented higher P_F with increasing pH and salt concentration. However, Y was not significantly affected by the variables under study. SDS showed only one dense band in the eluted fraction. Sulf-cryogel has shown that it can be used with high Y and P_F and low cost in the LPO purification.

5. Acknowledgments

This work was supported by the Coordination of Improvement of Higher Level Personnel (CAPES).

6. References

ATASEVER, A.; OZDEMIR, H.; GULCIN, I.; KUFREVIOGLU, O. I. One-step purification of lactoperoxidase from bovine milk by affinity chromatography. **Food Chemistry**, v. 136, n. 2, p. 864–870, 2013.

BARBOSA, L. C. A. Infrared spectroscopy: in the characterization of organic compounds. **Minas Gerais**, p. 189, 2007.

BRADFORD, M. M. A rapid and sensitive method for the quantitation of microgram quantities of protein utilizing the principle of protein-dye binding. **Analytical Biochemistry.** v. 72, p. 248–254, 1976.

CARVALHO, B. M. A.; DA SILVA, S. L.; DA SILVA, L. H. M.; MINIM, V. P. R.; DA SILVA, M. C. H.; CARVALHO, L. M.; MINIM, L. A. Cryogel Poly(acrylamide): Synthesis, Structure and Applications**. Separation & Purification Reviews**, v. 43, p. 241–262, 2014.

COIMBRA, J. C.; MARTINS, M. A.; MINIM, L. A. A simplified CFD model to describe fluid dynamics, mass transport and breakthrough curves performance in cryogel supports for chromatographic separation. **Chemical Engineering Research and Design**, v. 179, p. 56-65,

2022.

CHIU, C. K.; ETZEL, M. R. Fractionation of Lactoperoxidase and Lactoferrin from Bovine Whey Using a Cation Exchange Membrane ABSTRACT. **Journal of Food Science**, v. 62, n. 5, p. 996–1000, 1997.

DE OLIVEIRA, A. C. F.; NEVES, I. C. O.; SARAIVA, J. A. M.; DE CARVALHO, M. F. F.; BATISTA, G. A.; VERÍSSIMO, L. A. A.; RESENDE, J. V. DE. Capture of lysozyme on macroporous cryogels by hydrophobic affinity chromatography. **Separation Science and Technology**, v. 55, n. 11, p. 2012–2024, 2019.

GONÇALVES, G. R. F.; GANDOLFI, O. R. R.; SANTOS, C. M. S.; BONOMO, R. C. F.; VELOSO, C. M.; FONTAN, R. DA C. I. Development of supermacroporous monolithic adsorbents for purifying lectins by affinity with sugars. **Journal of Chromatography B**, v. 1033–1034, p. 406–412, 2016.

FONTAN, R. DA C. I.; BONOMO, R. C. F.; GONÇALVES, G. R. F.; MINIM, V. P. R.; MINIM, L. A. Alternatives for characterizing macroporous polyacrylamide monolithic ion exchanger columns. **Polymer Engineering Science**, v. 58, 2018.

GUIOCHON, G. The limits of the separation power of unidimensional column liquid chromatography. **Journal of Chromatography A**, v. 1126, p. 6–49, 2006.

JACOB, B. M., MANOJ, N. K., HARRIDAS, M. Antibacterial property of goat milk lactoperoxidase. **Indian Journal of Experimental Biology**, 36, 808–810, 1998.

JAIN, A.; BAJPAI, J.; BAJPAI, A. K. Structural, morphological and thermal characterization of poly (2-hydroxyethyl methacrylate-co-acrylonitrile) (P (HEMA-co-AN)) Cryogels: evaluation of water sorption potential and cytotoxicity. **Journal of Polymer Research**, v. 24, n. 7, 1 jun. 2017.

KUSSENDRAGER, K. D.; VAN HOOIJDONK, A. C. M. Lactoperoxidase: physico-chemical properties, occurrence, mechanism of action and applications. **British Journal of Nutrition**, v. 84, n. S1, 2000.

MORITA, Y.; ONO, A.; SERIZAWA, A.; YOGO, K.; ISHIDA-KITAGAWA, N.; TAKEYA, T.; OGAWA, T. Purification and identification of lactoperoxidase in milk basic proteins as an inhibitor of osteoclastogenesis. **Journal of Dairy Science**, v. 94, p. 2270–2279, 2011.

LAEMMLI, D. K. Cleavage of structural proteins during the assembly of the head of bacteriophage T4. **Nature**, 227, 680–685, 1970.

LEVENSPIEL, O. Chemical reaction engineering. **Industrial and Engineering Chemistry Research**, v. 38, n. 11, p. 4140–4143, 1999.

MACIEL, K. S.; SANTOS, L. S.; BONOMO, R. C. F.; VERISSIMO, L. A. A.; MINIM, V. P. R.; MINIM, L. A. Purification of lactoferrin from sweet whey using ultrafiltration followed by expanded bed chromatography. **Separation and Purification Technology**, v. 251, p. 117324, 2020.

MAHDI, L., MAHDI, N.; AL-KAKEI S.; MUSAFER, H.; AL-JOOFY, I.; ESSA, R.; ZWAIN, L.; SALMAN, I.; MATER, H.; AL-ALAK, S.; AL-OQAILI, R. Treatment strategy by lactoperoxidase and lactoferrin combination: Immunomodulatory and antibacterial activity against multidrug-resistant Acinetobacter baumannii. **Microbial Pathogenesis**, v. 114, n. November 2017, p. 147–152, 2018.

MARCUZ, C.; ALVES MOURÃO, C.; HAUPT, K.; ALVES BUENO, S. M. Performance of phospho-L-tyrosine immobilized onto alginate/polyacrylamide-based cryogels: Effect of ligand coupling on human IgG adsorption and Fab fragments separation. **Journal of Chromatography B**, 1165, 122530, 2021.

MÓL, P. C. G.; VERÍSSIMO, L. A. A.; ELLER, M. R.; MINIM, V. P. R.; MINIM, L. A. Development of an affinity cryogel for one step purification of lysozyme from chicken egg white, **J. Chromatogr. B Anal. Technol. Biomed. Life Sci.** 17–23, 1044–1045, 2017.

MÓL, P. C. G.; VERÍSSIMO, L. A. A.; MINIM, L. A.; BOSCOLO, M.; GOMES, E.; DA SILVA, R. Production and capture of β-glucosidase from Thermoascus aurantiacus using a tailor made anionic cryogel. **Process Biochemistry**, v. 82, p. 75–83, 1 jul. 2019.

NEVES, I. C. O.; RODRIGUES, A. A.; VALENTIM, T. T.; MEIRA, A. C. F. O.; SILVA, S. H.; VERÍSSIMO, L. A. A.; RESENDE, J. V. Amino acid-based hydrophobic affinity cryogel for protein purification from ora-pro-nobis (Pereskia aculeata Miller) leaves. **Journal of Chromatography B**, v. 1161, p. 122435, 15 dez. 2020.

PAN, M.; SHEN, S.; CHEN, L.; DAI, B.; XU, L.; YUN, J.; YAO, K.; LIN D-Q.; YAO, S-J. Separation of lactoperoxidase from bovine whey milk by cation exchange composite cryogel embedded macroporous cellulose beads. **Separation and Purification Technology**, v. 147, p. 132–138, 2015.

SAVINA, I. N.; GALAEV, I. Y.; MATTIASSON, B. Anion-exchange supermacroporous monolithic matrices with grafted polymer brushes of N,N-dimethylaminoethyl-methacrylate. **Journal of Chromatography A**, v. 1092, p. 199–205, 2005.

SINGH, P. K.; SHARMA, P.; BHUSHAN, A.; KAUR, P.; SHARMA, S.; SINGH, T. P. Structure of a ternary complex of lactoperoxidase with iodide and hydrogen peroxide at 1.77 Å resolution. **Journal of Inorganic Biochemistry**, 220, 111461, 2021.

URTASUN, N.; BAIELI, M. F.; HIRSCH, D. B.; MARTÍNEZ-CERON, M. C.; CASCONE, O.; WOLMAN, F. J. Lactoperoxidase purification from whey by using dye affinity chromatography. **Food and Bioproducts Processing**, v. 103, n. 1113, p. 58–65, 2017.

URTASUN, N.; MIGNON, A.; MARTÍNEZ-ALVAREZ, L. M.; BAIELI, M. F.; HIRSCH, D. B.; CASCONE, O.; DUBRUEL, P.; WOLMAN, F. J. Synthesis and characterization of chitosan mini-spheres with immobilized dye as affinity ligand for the purification of lactoperoxidase and lactoferrin from dairy whey. **Separation and Purification Technology**, v. 255, p. 117700, 15 jan. 2021.

VAN HOOIJDONK, C. M.; KUSSENDRAGER, K. D.; STEIJNS, J. M. In vivo antimicrobial and antiviral activity of components in bovine milk and colostrum involved in non-specific defence. **The British journal of nutrition**, v. 84 Suppl 1, n. 6, p. S127–S134, 2000.

VERÍSSIMO, L. A. A.; PAGANOTO, F. S.; MOL, P. C. G.; ILHÉU FONTAN, R. DA C.; MINIM, V. P. R.; MINIM, L. A. Preparation of an affinity cryogel column for lysozyme purification. **Separation Science and Technology.** 52, 2017.

YADAV, J. S. S.; YAN, S.; PILLI, S.; KUMAR, L.; TYAGI, R.D.; SURAMPALLI, R. Y. Cheese whey: A potential resource to transform into bioprotein, functional/nutritional proteins and bioactive peptides. **Biotechnology Advances**, v. 33, n. 6, p. 756–774, 2015.

YAO, K.; YUN. J.; SHAOCHUAN, S.; WANG, L.; HE, X.; YU, X. Characterization of a novel continuous supermacroporous monolithic cryogel embedded with nanoparticles for protein chromatography. **Journal of Chromatography A**, v. 1109, p. 103–110, 2006.

CONCLUSÕES

Este estudo propôs o desenvolvimento de novas estratégias de purificação das proteínas lactoferrina e lactoperoxidase do soro de leite. Os suportes utilizados foram meios macroporosos, uma vez que permitem o escoamento de soluções particuladas e mais viscosas sem que ocorra sua obstrução.

O modelo de Langmuir foi ajustado as isotermas de adsorção e a capacidade máxima de adsorção foi a pH 7,0 e 0,0 mM de NaCl. Em relação às propriedades hidrodinâmicas do leito expandido, verificou-se que o concomitante aumento do fluxo e da viscosidade da fase móvel afetou negativamente na dispersão axial e na capacidade dinâmica de ligação.

O soro de leite teve um volume reduzido de mais de 10 vezes pela ultrafiltração seguido de diafiltração. A lactoferrina apresentou em uma pureza de 92,7% e uma recuperação de 87,0% após a adsorção em leito expandido.

O criogel ativado com p-aminobenzenosulfonamida para adsorção específica da lactoperoxidase mostrou propriedades hidrodinâmicas e morfológicas de acordo com as características usuais. A capacidade de adsorção da lactoperoxidase foi afetada pela velocidade da fase móvel, sendo a melhor condição de 0,9 cm/min. Após a adsorção da lactoperoxidase, o fator de purificação aumentou em mais de 100 vezes e o rendimento foi de 100%, mostrando a alta especificidade da coluna de afinidade. SDS-PAGE mostrou-se uma única banda na fração eluída.

Diante do exposto, os dois modelos propostos foram eficientes na obtenção da lactoferrina e da lactoperoxidase do soro de leite, com alta pureza e recuperação.